3D VIRTUAL SIGHT DISTANCE ANALYSIS USING LIDAR DATA

FINAL PROJECT REPORT

by

Michael J. Olsen (PI)
David S. Hurwitz (Co-PI)
Alireza G. Kashani (Co-PI)
Kamilah Buker
Oregon State University

Disclaimer

The contents of this report reflect the views of the authors, who are responsible for the facts and the accuracy of the information presented herein. This document is disseminated under the sponsorship of the U.S. Department of Transportation's University Transportation Centers Program, in the interest of information exchange. The Pacific Northwest Transportation Consortium, the U.S. Government and matching sponsor assume no liability for the contents or use thereof.

Technical Report Documentation Page

1. Report No.	2. Government Accession No.	3. Recipient's Catalog No.

4. Title and Subtitle	5. Report Date
3D Virtual Sight Distance Analysis Using Lidar Data	October 7, 2016
	6. Performing Organization Code

7. Author(s)	8. Performing Organization Report No.
Michael J. Olsen, David S. Hurwitz, Alireza G. Kashani, Kamilah Buker	

9. Performing Organization Name and Address	10. Work Unit No. (TRAIS)
PacTrans	
Pacific Northwest Transportation Consortium	**11. Contract or Grant No.**
University Transportation Center for Region 10	
University of Washington More Hall 112 Seattle, WA 98195-2700	

12. Sponsoring Organization Name and Address	13. Type of Report and Period Covered
United States of America	
Department of Transportation	**14. Sponsoring Agency Code**
Research and Innovative Technology Administration	

15. Supplementary Notes

Report uploaded at www.pacTrans.org

16. Abstract

This research project investigated advanced safety analysis methodologies for drivers' sight distance based on high resolution data acquired using lidar (light detection and ranging) technology. Sight distance analyses require careful and detailed field measurements to facilitate proper engineering decision making regarding the removal of obstructions, establishment of regulatory and advisory speed limits, and the location of new access points, among numerous other examples. However, conventional field measurements present safety concerns because they require personnel to be in or adjacent to traffic lanes. They can also be time consuming, costly, and labor intensive. Furthermore, the predominantly two-dimensional (2D) methods involve simplifying assumptions such as a "standard" vehicle heights and lengths without considering the wide range of vehicles and drivers present on the road. Recently, departments of transportation have begun to acquire mobile lidar data for their roadway assets. As an example, Oregon DOT has recently completed scan surveys of all state owned and maintained highways and updates of high priority areas annually. These data provide a rich, three-dimensional (3D) environment that enables one to virtually visit a site at any frequency and efficiently evaluate sight distances from the safety of the office. This research presents a systematic processing and analysis workflow for virtually evaluating available sight distances by using lidar data sets named SiDAL (Sight Distance Analysis using Lidar). This approach enables one to repeatedly analyze the same scene whle considering a variety of vehicle types as well as multi-modal forms of transportation (e.g., bikes, pedestrians). The sensitivity of this technique to modeling resolution was analyzed by using a case study of an intersection with restricted visibility. The results showed the ability to capture significantly more detail about visibility constraints in comparison to conventional measurements.

17. Key Words	18. Distribution Statement
Sight Distance, Safety, lidar, laser scanning, visibility, visualization	No restrictions.

19. Security Classification (of this report)	20. Security Classification (of this page)	21. No. of Pages	22. Price
Unclassified.	Unclassified.		NA

Form DOT F 1700.7 (8-72) **Reproduction of completed page authorized**

Table of Contents

List of Figures

List of Tables

List of Abbreviations

$\triangle$: User-defined grid size, voxel size
2D: Two-dimensional
3D: Three-dimensional
ALS: Airborne Laser Scanning
ASD: Available Sight Distance
DEM: Digital Elevation Model
DM: Digital Model
DSM: Digital Surface Model
GIS: Geographic Information Systems
GPS: Global Positioning System
GNSS: Global Navigation Satellite System
ISD: Intersection Sight Distance
Lidar: Light detection and ranging
LOS: Line of Sight
MLS: Mobile Laser Scanning
ODOT: Oregon DOT
ORGN: Oregon Real-Time GPS Network
PacTrans: Pacific Northwest Transportation Consortium
SiDAL: Sight Distance Analysis using Lidar
SD: Sight Distance
SSD: Stopping Sight Distance
STLS: Static Terrestrial Laser Scanning
TIN: Triangulated Irregular Network
VR: Virtual Reality

Acknowledgments

Executive Summary

This research project investigated advanced safety analysis methodologies for drivers' sight distance based on high resolution data acquired with lidar (light detection and ranging) technology. Sight distance analyses require careful and detailed field measurements to facilitate proper engineering decision making regarding the removal of obstructions, establishment of regulatory and advisory speed limits, and the location of new access points, among numerous other examples. However, conventional field measurements present safety concerns because they require personnel to be in or adjacent to traffic lanes. They can also be time consuming, costly, and labor intensive. Furthermore, the predominantly two-dimensional (2D) methods involve simplifying assumptions such as a "standard" vehicle heights and lengths without considering the wide range of vehicles and drivers present on the road.

Recently, departments of transportation (DOTs) have begun to acquire mobile lidar data for their roadway assets. As an example, Oregon DOT (ODOT) has recently completed scan surveys of all state owned and maintained highways and updates of high priority areas annually. These data provide a rich, three-dimensional (3D) environment that enables one to virtually visit a site at any frequency and efficiently evaluate sight distances from the safety of the office.

This research presents a systematic processing and analysis workflow for virtually evaluating available sight distances by using lidar data sets named SiDAL (Sight Distance Analysis using Lidar). This approach enables one to repeatedly analyze the same scene while considering a variety of vehicle types as well as multi-modal forms of transportation (e.g., bikes, pedestrians). The sensitivity of this technique to modeling resolution was analyzed by using a case study of an intersection with restricted visibility. The results showed the ability of the SiDAL approach to capture significantly more detail about visibility constraints in comparison to conventional measurements.

This is **an intentionally blank page**.

Chapter 1 Introduction

A key component in the safe design, operation, and maintenance of highways is the provision of adequate sight distance (SD). SD is the length of road visible to a road user measured from any point along the traveled way. Sight distance analyses require careful and detailed field measurements to facilitate proper engineering decision making regarding the removal of obstructions, establishment of regulatory and advisory speed limits, and the location of new access points, among numerous other examples. Transportation facilities should be designed such that a driver has sufficient visibility to avoid collision with an object obstructing the traveled way. SD measurements and calculations are based on driver characteristics, vehicle types, road grade, horizontal and vertical curves in the road, road conditions (e.g., wet surfaces), and the type of maneuver that the driver will perform.

Limited visibility is a principal cause of accidents in transportation corridors and construction sites. A study of construction fatalities from 1990 to 2007 determined that lack of visibility is a primary cause in approximately 5 percent of cases. The findings also showed that when equipment and a vehicle were involved in a fatality, over 23 percent of the incidents were the result of obstructions (Hinze & Teizer, 2011). Investigation of these cases showed that specific preventive safety practices could reduce the number of these fatalities. One solution is to identify obstacles and hazardous road or construction work spaces, which will allow for the selection of proper strategies such as removing obstructions, implementing safety warning signs, and optimizing blind spaces by alternating the road or construction site features and equipment locations.

1.1 Limitations of Current Sight Distance Measurements

Conventional field measurements of SD present safety concerns because they require personnel to be in or adjacent to active traffic lanes. These studies are generally time consuming,

costly, and labor intensive. Furthermore, the methods that are currently used are based on 2D theoretical equations, which require simplifying assumptions such as a "standard" vehicle (height and length) without considering the wide range of vehicles present on the road. Another limitation in conventional SD analyses is that only static objects and vehicles are considered. This approach does not enable one to model the dynamic motions of both vehicles and objects that occur in the real world.

1.2 Potential of Mobile Lidar Data

Lidar is a recent technology that can rapidly generate survey quality, three-dimensional (3D) data of a scene, which can be utilized to analyze visibility within a space. A key benefit to lidar technology is the ability to utilize the same data source to support multiple applications, including asset management, safety analyses, construction, planning, and maintenance. Lidar data provide a 3D environment that enables one to frequently virtually visit a site and efficiently obtain measurements from the safety of the office.

Recently, departments of transportation (DOTs) have begun to acquire mobile lidar data for their highways. NCHRP Report #748 "Guidelines for the use of mobile lidar in transportation applications" (Olsen et al. 2013) is a comprehensive resource for learning about mobile lidar technology and implementing it for transportation applications. The material from this report has been incorporated into an e-learning website, http://learnmobilelidar.com.

As an example, Oregon DOT (ODOT) has recently completed scan surveys of all state-owned and maintained highways and updates of high priority areas annually. ODOT was able to utilize these data to perform virtual passing sight distance analyses of rural highways where speed limit increases were introduced. The State of Oregon decided to increase the speed limits on these highways and needed to determine whether passing lane markings were adequate for the increased speed. Use of mobile laser scanning (MLS)

provided a safer, more efficient, and more cost-effective solution to acquiring these data in comparison to traditional techniques.

Recently, with the trend toward autonomous vehicles, lidar technology has been incorporated into some vehicles as part of a collision avoidance system, where the vehicle continually scans for objects in its path.

1.3 Research Objectives and Scope

This research explored the feasibility, benefits, and challenges of using a safety analysis for sight distances based on DOT laser scanning data. Specifically, the following objectives were accomplished:

➢ develop a systematic framework to utilize laser scanning data to evaluate sight distances in different, practical scenarios, such as drivers approaching a signalized intersection

➢ evaluate the sensitivity of the analysis approach to user input parameters, and

➢ compare the new methodology to conventional techniques for validation, focusing on improvements in efficiency, safety, and data quality.

Chapter 2 Literature Review

To strengthen the argument for the above-mentioned research focus, a brief review of

literature relevant to sight distance analysis is provided. The information regarding DOT

standards provided in this literature review was taken from states located in and around Oregon.

Standards in the Midwest and along the East Coast may differ.

2.1 Sight Distance Determination

The AASHTO Green Book (AASHTO 2011) defines SD as "the length of roadway

ahead that is visible to the driver." For the safe and efficient operation of a vehicle, a driver must

have the ability to see ahead and have sufficient SD to avoid colliding with unexpected objects.

The determination of SD depends on the height of the driver's eye above the roadway,

the specified object height above the road surface, and the height and lateral position of sight

obstructions within the driver's line of sight (AASHTO 2011). For all SD calculations of

passenger vehicles, the height of the driver's eye is assumed to be 1.08 meters (3.50 feet) above

the road surface. At every point along a roadway, the SD should be suitably long enough for a

shorter than average driver or vehicle traveling at or near the design speed to stop before a

collision occurs.

Nonetheless, it is important to recognize that drivers may travel faster than the design or

posted speed when performing these SD analyses (AASHTO 2011). Speed can be utilized both

as a design criterion to promote consistency and a performance measure for evaluating designs of

highways and streets (Fitzpatrick 2003). The design speed concept was developed under the

assumption that it represents the maximum reasonable, uniform speed of the group of faster

driving vehicles (Fambro et al. 2007). However, recent studies have discovered that design

speed no longer represents the speed adopted by the faster driving groups of vehicle operators,

but, rather, it is now used to correlate design elements and represents a maximum safe speed (Fambro et al. 2007). Regardless, design speed has minimal impact on the actual operating speeds (Fitzpatrick 2003), where operating speed is the speed at which vehicles move during free flow conditions (FHWA, n.d).

There is a strong limitation associated with calculations that use a single speed as an input variable because of the variability in operating speed that exists for a given design speed, posted speed, or a set of roadway characteristics (Fitzpatrick 2003). The National Highway Cooperation Research Program (NCHRP) conducted a study on stopping sight distance (SSD) by measuring operating speed on a limited SD crest vertical curve and discovered that as the inferred design speed increased, operating speeds were higher (Fitzpatrick 2003). The study found that, in general, the lower the design speed, the larger the differential was between the observed operating speed and the design speed (Fambro et al. 2007).

Two aspects of SD are discussed in this review: SSD and intersection sight distance (ISD). SSD is defined as the sum of the distance traversed by the vehicle from the instant the driver detects an object obstructing the forward progression of the vehicle on the current path necessitating the driver to stop to the instant the brakes are applied (brake reaction distance) and the distance needed to stop the vehicle once the brakes have been applied (braking distance). In addition to SSD, SD must also be considered at intersections (commonly termed ISD) to provide drivers of stopped vehicles an adequate view of the intersecting highway to allow them to cross or enter the intersecting highway.

For SSD, the object considered is 0.60 meters (2.00 feet) or more above the roadway surface; whereas ISD is based on a vehicle located 15 feet back from the fog line/edge of the traveled way to an object in the highway (McKinley 2011) with a height of 1.08 meters (3.50 feet) (AASHTO 2011).

2.1.1 Stopping Sight Distance Variables and Calculation (SSD)

SSD is the minimum length of unobstructed roadway sufficient enough for a driver to identify an object in the roadway and have the ability to stop in order to avoid a collision (McKinley 2011). In most conditions, the driver must have the ability to both see the object and recognize that it is stationary or slow moving against the background of the roadway or other sceneries (AASHTO 2011). To determine the required SSD, seven variables must be considered: perception reaction time (PRT), driver eye height, object height, vehicle operation speed, pavement coefficient of friction, deceleration rates, and the roadway grade (Transportation Research Institute 1997a).

As stated in the previous section, SSD is the sum of the brake reaction distance and the braking distance. The recommended design criteria for the brake reaction time is 2.5 seconds for SSD (AASHTO 2011). This brake reaction time surpasses the 90th percentile of reaction time for all drivers and comprises the capabilities of most drivers. The 2.5-second brake reaction time is sufficient for complex driving conditions but is not adequate for the most complex conditions experienced in actual driving (AASHTO 2011). The distance travelled during the brake reaction time can be calculated by the equations displayed in figure 2.1.

Metric	**US Customary**
$d = 0.278Vt + 0.039 \dfrac{V^2}{a}$	$d = 1.47Vt + 1.075 \dfrac{V^2}{a}$

Where:
   t = brake reaction time, 2.5 s;
   V = design speed, km/h; a =
   deceleration rate, m/s^2
	Where:
	   t = brake reaction time, 2.5 s;
	   V = design speed, mph; a =
	   deceleration rate, ft/s^2

Figure 2.1 SSD equation for calculating the distance travelled during the brake reaction time. (AASHTO 2011)

The braking distance of a vehicle on a level roadway traveling at the design speed of the

roadway is calculated by the equations displayed in figure 2.2 (AASHTO, 2011):

Metric	US Customary
$$d = 0.039 \, \frac{V^2}{a}$$	$$d = 1.075 \, \frac{V^2}{a}$$

Where:
  d = brake reaction time,
  m; V = design speed,
  km/h; a = deceleration
  rate, m/s^2
	Where:
	  d = brake reaction time,
	  ft; V = design speed, mph;
	  a = deceleration rate, ft/s^2

Figure 2.2 Braking distance equations (AASHTO 2011)

The recommended deceleration rate for determining SSD is 3.4 m/s^2 (11.2 ft/s^2)

(AASHTO 2011). This rate is sufficient for drivers to decelerate comfortably while maintaining

the ability to stay within their lane as well as steering control during the braking process on wet

surfaces (AASHTO 2011). It is assumed that most vehicle braking systems and tire-pavement

friction levels of most roadways have the capability of providing the given deceleration rate

(AASHTO 2011).

2.1.2 Intersection Sight Distance Variables and Calculation (ISD)

ISD is a major contributor to the safet operation of roadways (Transportation Research

Institute 1997b). Each and every intersection has the potential to encounter several different

types of vehicular conflicts (AASHTO, 2011). These conflicts can be significantly reduced with

the provision of suitable SD. ISD is defined as the minimum length of an unobstructed line of

sight between a vehicle entering an intersection or highway and the vehicles approaching

(McKinley 2011). Sufficient ISD allows drivers of stopped vehicles an adequate view of the

intersecting highway to decide when to enter or cross the intersecting highway, while still

allowing traffic on the given highway to maintain a normal travel speed (McKinley 2011). When the available SD for an entering/crossing vehicle is equal to the SSD of the major road, then drivers will have appropriate SD to anticipate and avoid collisions (AASHTO 2011). When the ISD is greater than the SSD along a major roadway, traffic operations are significantly improved (AASHTO 2011).

Clear sight triangles are specified areas along intersection approach legs that should be clear of obstructions to allow a driver to view potential conflicting vehicles (AASHTO 2011). The dimensions of the legs for a sight triangle depend on the traffic control type and the design speeds of the given intersecting roadway. There are two types of sight triangles considered when determining the intersection sight distance: approach and departure. For approach sight triangles, each quadrant of an intersection should contain triangular areas free of obstructions. The length of the legs of these triangular areas should be appropriately designed to allow drivers to see any potential conflicting vehicles with adequate time to slow or stop before colliding within the intersection. A departure sight triangle provides a sufficient sight distance to allow a stopped driver on a minor road approach to depart from the intersection and either enter or cross the intersection. Figure 2.3 shows diagrams for both approach and departure sight triangles.
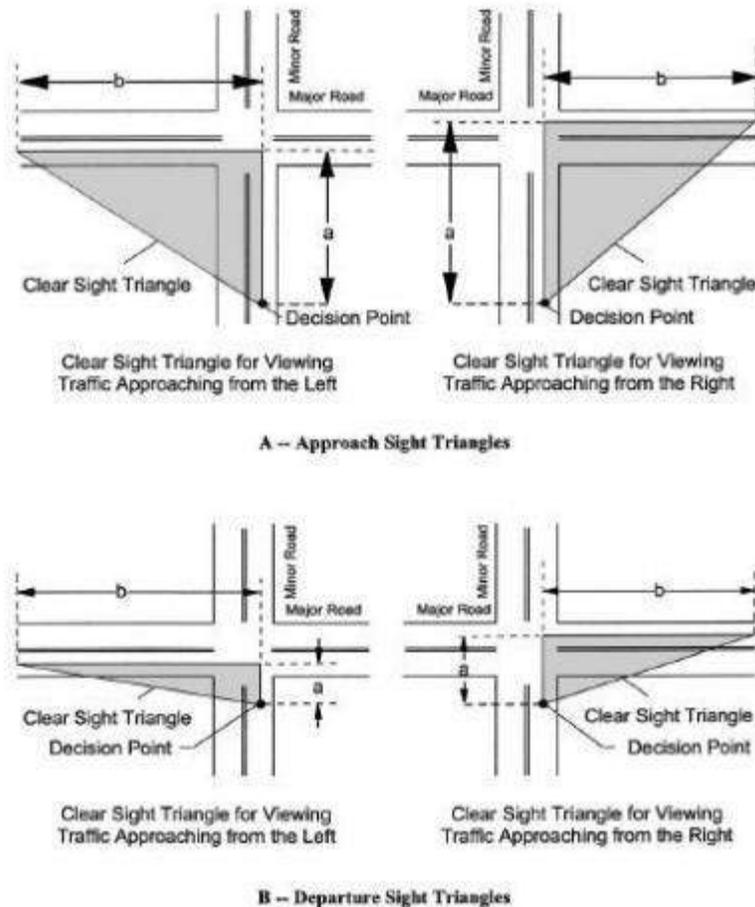
Figure 2.3 Intersection sight triangles (from AASHTO 2011)

AASHTO (2011) defines *a* as the distance from the major road along the minor road. The distance of *b* describes the length of the leg of the sight triangle. Within sight triangles, any object above the height of the adjacent roadway that has the potential to obstruct the driver's view should be removed or lowered. The determination of whether an object constitutes a sight obstruction is based on the assumption that the driver's eye height is 1.08 meters (3.50 feet) above the roadway and that the object is 1.08 meters (3.50 feet) above the surface of the intersecting roadway. The object height is based on a vehicle height of 1.33 meters (4.5 feet).

Utilizing an object height equal to the driver height ensures that the ISD is reciprocal (AASHTO 2011). The following equations (figure 2.4) are used to calculate ISD along a major roadway.

Metric	US Customary
$$ISD = 0.278V_{major}t_g$$	$$d = 1.47Vt + 1.075\,\frac{V^2}{a}$$

Where:
   ISD = intersection sight distance (length of the leg of sight triangle along the major road) (M)
   V_{major} = design speed for minor road (km/h);
   t_g = time gap for minor road vehicle to enter the major road (s)
	Where:
	   ISD = intersection sight distance (length of the leg of sight triangle along the major road) (ft)
	   V_{major} = design speed for minor road (mph);
	   t_g = time gap for minor road vehicle to enter the major road (s)

Figure 2.4 Intersection sight distance equations (AASHTO 2011)

The time gap for a passenger car turning left onto a two-lane major road is recommended to be 7.5 seconds and 8.0 seconds for a four-lane major road (AASHTO 2011). If the intersection is located on a 4 percent upgrade, the time gap selected should be 8.8 seconds (a 0.2-second increase for each percentage increase in grade).

2.1.3 Field SD Measurements

AASHTO (2011) states that "[SD] should be considered in the preliminary stages of design when both the horizontal and vertical alignment are still subject to adjust." The early incorporation of SD enables the designer to create a more balanced design by making minor adjustments to the plan and profileSD along the centerline or traveled-way edge. Figure 2.5 (AASHTO 2011) shows the process of measuring and recording of SD for design plans. Other DOTs (e.g., ODOT) provide similar drawings in their highway design manuals.
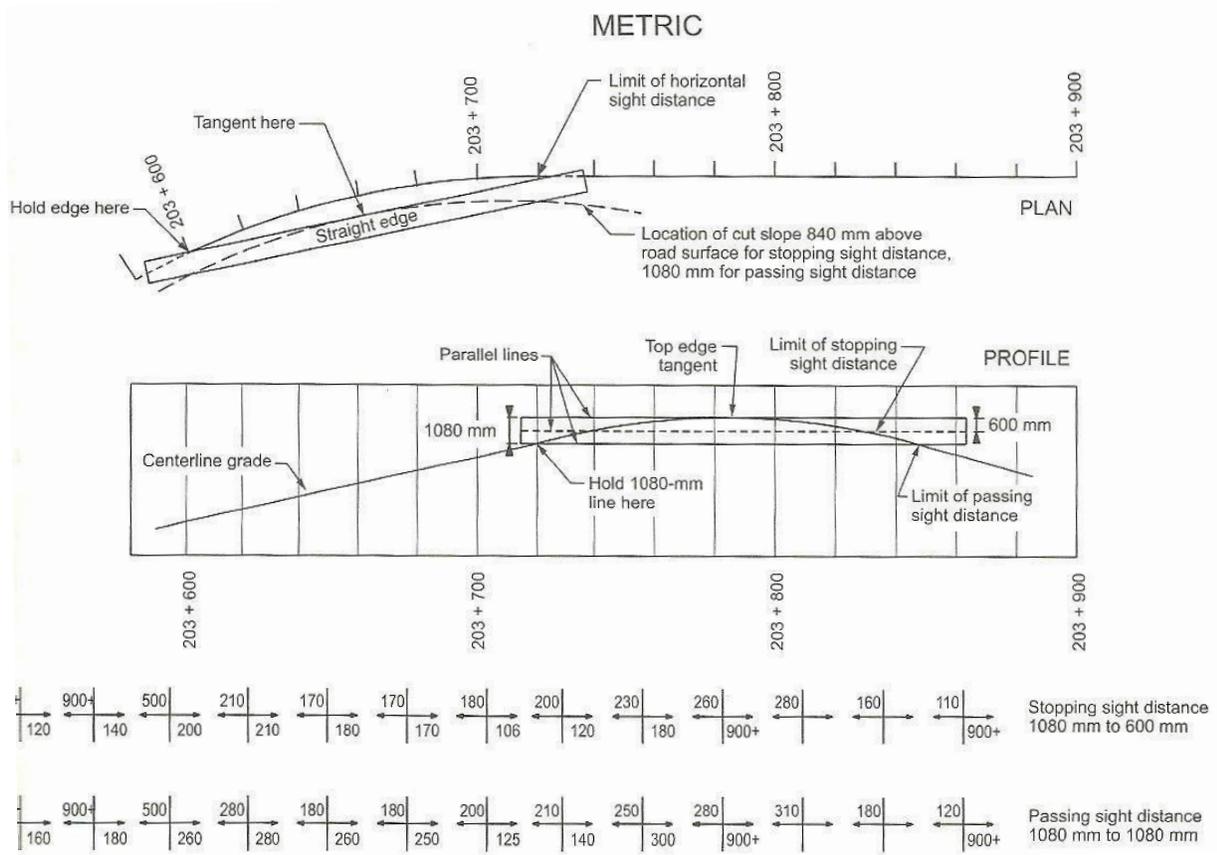
Figure 2.5 Scaling and recoding SD on plans (AASHTO 2011)

Each state DOT has its own methodologies for measuring sight distance. For example, the Oregon Department of Transportation (ODOT) states that, at a minimum, the stopping sight distance must be obtained on the vertical and horizontal alignments of the road (ODOT 2012). The horizontal sight distance must at least equal the SSD and is measured 0.61 meters (2 feet) above the centerline of the inside lane at the point of obstruction (ODOT 2012).

Like ODOT, the California Department of Transportation (Caltrans) assumes that the line of sight intercepts the view obstruction at the midpoint of the sight line and is located 2 feet above the center of the inside lane when the road profile is flat (Caltrans 2014b). The clear distance is measured from the center of the inside lane to the obstruction. The

Washington State Department of Transportation (WSDOT) measures the horizontal sightline offset from the centerline of the inside lane of the curve to the sightline obstruction (WSDOT 2013).

The Idaho Department of Transportation (ITD) conducted a study to measure existing roadway conditions in Idaho at various US 89 intersections. Similar to the ODOT procedure, ITD also records the posted speed limit when measuring SD in the field (ITD 2007).

2.1.1 Oregon DOT's SD procedure

To measure SD in the field, ODOT posted a *Technical Services Bulletin* that describes its four-step procedure to measure SD at intersections with a stop control at the approach (McKinley 2014). First, crews record the number of lanes on the highway followed by the widths. Next, they measure the roadway grades with a Smartlevel at the steepest section within 900 to 1,500 feet left and right of the intersection and record the posted speed.

To measure SD (the final step), four objects are set up in line with the center of the proposed intersection (McKinley 2014). Figure 2.6 shows the placement of each object and a detailed diagram of the procedure for measuring sight distance at intersections with a stop control at the approach. Object 1 is located opposite of the fog stripe/curb at a height of 0.61 m (2.0 feet), and Object 2 is located near the fog stripe/curb with the same height. Objects 3 and 4 are located behind the near fog stripe/curb at a height of 1.07 m (3.5 feet) to represent the driver's height.
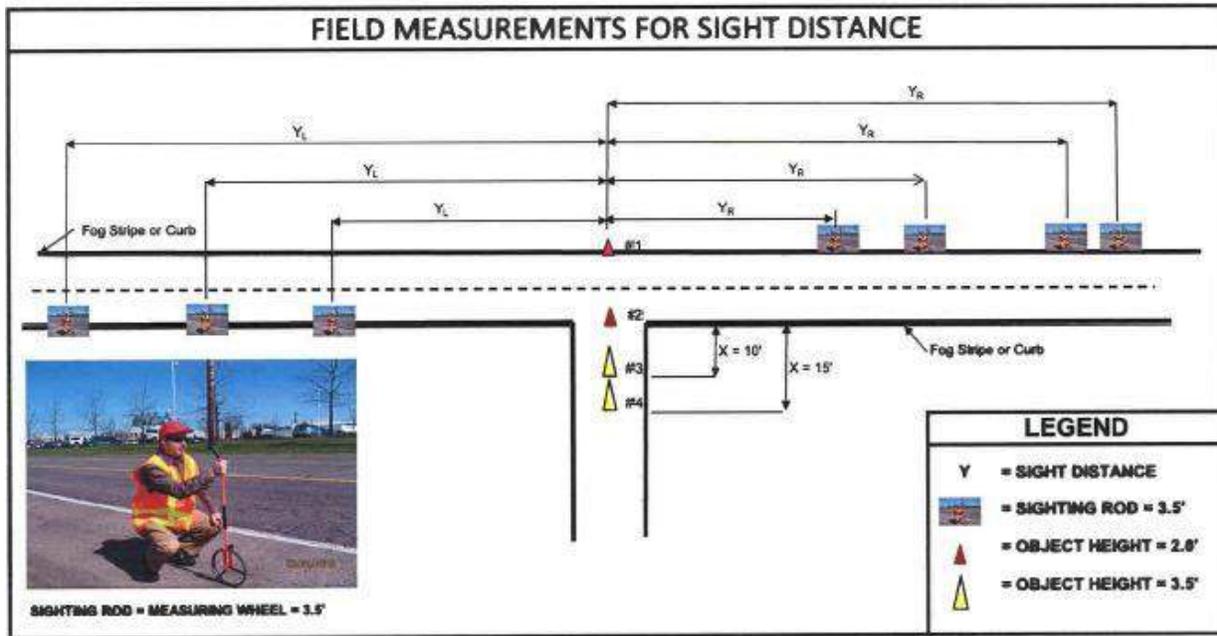
Figure 2.6 SD measurement procedure diagram (McKinley 2014)

All the measurements left are taken from the near fog stripe/curb, while all the measurements from the right are taken from the opposite fog stripe/curb (McKinley 2014). Starting on or near the fog stripe/curb and at the centerline of the approach, the crew sets the measuring wheel to 0 feet and walks along the roadway until they cannot see any of the markers. From there the distance is recorded. This process is continued for the remaining markers or until the maximum distance of 900 to 1500 feet is reached. The measurements from right of the approach are to objects 1, 2, 3, and 4. Measurements taken from the left of the approach are to objects 2, 3, and 4. The sight triangle is clear of obstructions if the distances measured to the objects are between 900 to 1500 feet. Larger distances are also acceptable.

2.1.2 State Practices

Despite the AASHTO (2011) recommended practices to calculate both SSD and ISD, many DOTs follow statewide design standards when considering the driver eye height and object

height for both SSD and ISD. ITD and the Arizona Department of Transportation (ADOT) both

directly refer to the *AASHTO Green Book* for standards regarding SSD and ISD.

2.1.3 Driver Height Standards

Table 2.1 displays the standard for driver eye height for Oregon and surrounding state

DOTs. Most DOTs around the United States have adopted a consistent standard of 3.50 feet as

the SSD and ISD driver eye height. Additional DOTs (not included in table 2.1) that also follow

the same standard for driver eye height are the Iowa Department of Transportation (Iowa DOT)

and the Texas Department of Transportation

(TxDOT).

Table 2.1 Driver eye height standards

Types of Sight Distance	ODOT	Caltrans	WSDOT	ADOT	ITD	AASHTO 2011
SSD	3.50 ft	3.50 ft	3.50 ft	3.50 ft	3.50 ft	3.50 ft
ISD	3.50 ft	3.50 ft	3.50 ft	3.50 ft	3.50 ft	3.50 ft

2.1.4 Object Height Standards

As with driver eye height, most DOTs follow the same standard for the object height.

Table 2.2 displays the object height standards for Oregon DOT and surrounding states.

Table 2.2 Object height standards

SD Type	ODOT	Caltrans	WSDOT	ADOT	ITD	AASHTO 2011
SSD	2.00 ft	0.50 ft	2.00 ft	2.00 ft	2.00 ft	2.00 ft
ISD	3.50 ft	4.25 ft	3.50 ft	3.50 ft	3.50 ft	3.50 ft

Caltrans has a significantly higher ISD standard for object height, which may be a result

of the equation used to determine it. Caltrans designs ISD by using a 7.50-second, horizontal SD

criterion (Caltrans 2001). Caltrans also assumes that the driver of the vehicle waiting at the

crossroad is set back a minimum of 10 feet plus the shoulder width of the major road and not less

than 15 feet total (Caltrans 2014a). However, if the major road has a median barrier, the standard

object height to be used is 2.00 feet in the median barrier set back.

2.1.5 Multi-Modal

Most DOTs provide these standards for passenger vehicles within their highway design

manuals. A few also provide standards for other modes of transportation, such as trucks and

bicycles. Not all DOTs provide recommendations for truck standards or other modes of

transportation. Table 2.3 provides SD standards for other modes of transportation from select

DOTs, including the Minnesota Department of Transportation (MnDOT and Colorado

Department of Transportation (CDOT).

Table 2.3 Other SD standard values

Types of Sight Distance	ODOT	Caltrnns	WSDOT	Iowa DOT	MnDOT	CDOT	AASHT0 2011
Truck driver height	7.60 ft	-	6.00 ft	7.60 ft	-	-	7.60 ft
Bicyclist eye height (SSD)	-	4.50 ft	-	-	4.50 ft	4.50 ft	-
Bicyclist object height (SSD)	-	0.33 ft (100 mm)	-	-	0.00 ft	0.00 ft	-

A similar review on SD (table 2.4) was conducted at Oregon State University (OSU) in

2012 by Robert Layton and Karen Dixon, entitled *Stopping Sight Distance.* Their study

compared the same DOTs to determine the differences between the standard driver eye heights

and object heights in the years 2001, 2009, and 2011 (Layton and Dixon 2012). The information

in this report was compiled from the DOTs from the year 2011 and on, except that Caltrans and

MnDOT bicyclist data were from 2006 and 2007.

Table 2.4 SD comparisons for object height (Layton and Dixon 2012)

	2001 & 20011 AASHTO	2009 CALTRANS	2001 ODOT	2011 WSDOT
Object for stopping sight distance	2.0 ft. (600 mm)	0.5 ft. (150 mm)	0.5 ft. (150 mm)	0.5 ft. (150 mm)
Object for decision sight distance	2.0 ft. (600 mm)	0.5 ft. (150 mm)	0.5 ft. (150 mm)	0.5 ft. (150 mm)
Object for passing sight distance	3.5 ft. (1080 mm)	4.25 ft. (1300 mm)	3.5 ft. (1080 mm)	3.5 ft. (1080 mm)
Object for intersection sight distance	3.5 ft. (1080 mm)	4.25 ft. (1300 mm)	3.5 ft. (1080 mm)	3.5 ft. (1080 mm)
Object for access drivers	2.0 ft. (600 mm)	-	-	-
Pavement (SSD)	0	-	-	-

2.2 Geospatial Technologies for SD Analysis

Recent geospatial approaches have been proposed to calculate available SD for road designs (Hassan et al. 1996, Ismail and Sayed 2007; Jha and Karri 2009; Jha et al. 2011). These methods use design alignments and terrain topographic information to simulate the road geometry and conduct SD calculations. However, a major limitation arises because these approaches only consider the road geometry and ignore the influence of other effective objects such as trees, buildings, signs, etc. Moreover, these methods simplify the road geometry (e.g., constant road grade and cross slope) with assumptions, which can vary significantly along a highway. Table 2.5 presents a summary of related studies.

Table 2.5 Summary of related studies performing geospatial visibility analyses

Reference	Publication	Contribution	GIS function	Model used	Lidar used
Khattak et al. (2003)	TRR	GIS LOS method to detect intersection SD obstructions	LOS	First and last return DTM	ALS
Khattak & Shamayleh (2005)	CCE	GIS viewshed method to detect a road SD obstructions	Viewshed	DSM	ALS
Tsai et al. (2011)	TRR	GIS POS method to detect intersection SD obstructions and quantify the severity	Viewshed	DSM	ALS
Castro et al. (2011)	TR part C	GIS viewshed method to calculate ASD on a highway	Viewshed	DTM	N/A
Castro et al. (2014)	CCE	GIS POS loops to calculate ASD on a highway and detect diving locations	LOS loop	DTM	N/A
Santos & Castro (2014) - Castro et al. (2015)	Procedia - Survey Review	Compare the influence of DTM and DSM made from ALS and MLS data on method presented in Castro et al. (2014)	LOS loop	DTM, DSM	ALS, MLS

Recent developments in Geographic Information Systems (GIS) and digital elevation modeling (DEM) provide efficient tools for road SD analysis. GIS enables the evaluation of available sight distance (ASD) on existing roads and intersections without the need for design alignments and data. GIS also enables one to combine SD analysis results with other sources of information such as crash statistics and speed limits for further evaluation.

Two main approaches for calculating ASD in GIS are to use viewshed (figure 2.7 (a)) and line of sight (LOS) (figure 2.7 (b)). Some methods use the ArcGIS LOS and viewshed analysis tools to determine ASD on roads (Khattak and Shamayleh, 2005; Castro et al. 2011; Castro et al. 2014) and intersections (Khattak et al. 2003; Tsai et al. 2011). In the viewshed approach, first assumptions such as vision range, angle, and obstacle locations are used to determine the driver

viewshed area (e.g., the polygon in figure 2.7 (a)). Then, the road section included in the

viewshed polygon is determined and the length of the ASD is extracted. In the LOS approach,

the line of sight is used to detect points on the road that can be seen by the driver. To calculate

ASD with this approach, path points are made on the GIS road trajectory polyline with equal

distances (e.g., A, B, C, and D in figure 2.7 (2)). Then the ASD is determined by calculating the

path distance between the driver point (e.g., A in figure 2.7 (2)) and the last seeable path point

(e.g., D in figure 2.7 (2)).
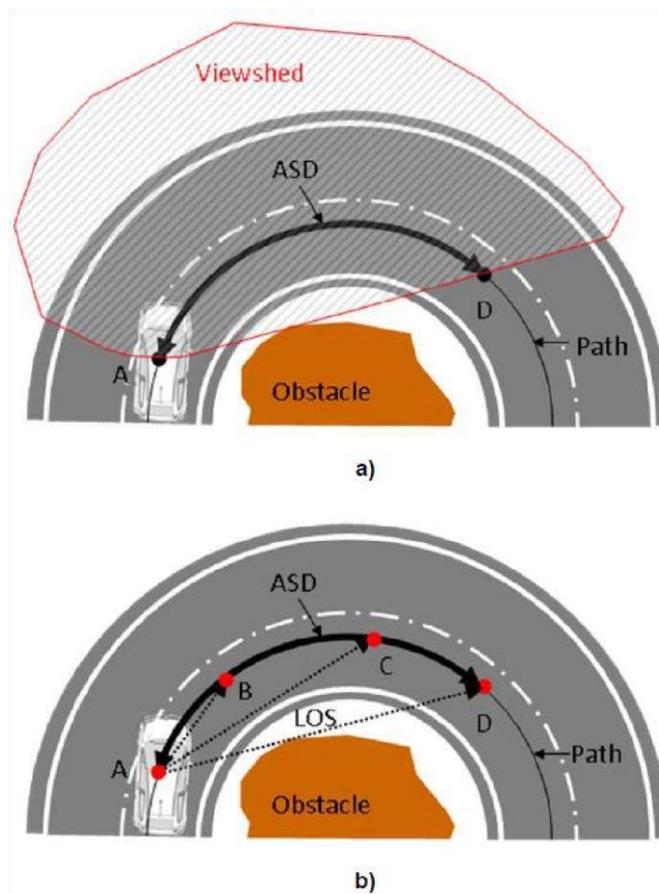
Figure 2.7 SD analysis in GIS (from Castro et al. (2015)) (a) viewshed approach, (b) LOS approach

2.2.1 Digital Models

The GIS-based methods require a digital model representing the geometry of the road and its environment. Two types of digital models used are digital elevation models (DEMs), sometimes referred to as digital terrain models (DTMs), and digital surface models (DSMs). DEMs represent the bare ground surface. However, DSMs are more beneficial for SD analysis because they include other on-the-ground objects such as trees, buildings, walls, and traffic signs that would create obstructions.

The digital models used in the current proposed methods are typically generated by using light detection and ranging (lidar) data. The type and resolution of lidar data collection can have a significant impact on SD analyses. Three common methods of lidar data collection include airborne laser scanning (ALS), mobile laser scanning (MLS), and static terrestrial laser scanning (sTLS). STLS and MLS provide point cloud data with higher density. MLS also can capture better views from vertical objects such as trees, signs, walls, etc. Therefore, DEMs derived from sTLS and MLS data often represent the road and roadside objects more realistically.

Note that the DSMs in current GIS methods do not fully represent the geometry of 3D objects, which can adversely influence the SD analyses by not accounting for visible space underneath some objects such as tree crowns, building overhangs, signs, power lines, and tunnels located above the road surface. DSMs can be represented as a triangulated irregular network (TIN) made by Delaunay triangulation. In this approach, first, only the horizontal projection of points is used to form non-overlapping triangles. Then, point elevations are added to build up the network. Unfortunately, this approach does not fully support a 3D representation of surfaces because it generates only non-overlapping surfaces when projected to 2D. Therefore, the resulting DSM cannot include surfaces with the same horizontal locations but different

elevations. Some references refer to such a method as 2.5 D instead of 3D (Santos and Castro, 2014).

2.2.2 Virtual Reality Assessments

Recent developments in 3D data collection, visualization, and virtual reality (VR) technologies could enhance safety practices. Three-dimensional data collection allows as-built geometry of roads and construction jobsites to be saved. VR environments enable exploration of the 3D representation of reality and interaction with virtual objects. Integration of these techniques will allow engineers and construction workers to virtually conduct measurements and work operations in an environment that replicates actual jobsite conditions without putting them at risk of injury. VR environments have been used recently in construction safety operations, including applications in safety training and education (Squelch, 2001; Zhao et al., 2009; Dickinson et al, 2011; Guo et al., 2012, Park and Kim, 2013), hazard identification and assessment (Lin et al., 2011; Chen et al., 2013).

Chapter 3 Study Site and Data Collection Procedures

3.1 Site Overview

The intersection of SW Jefferson Way and SW 9th Street (figure 3.1) is located in

Corvallis, Oregon, near Oregon State University. SW Jefferson Way runs east/west while SW

9th St. runs north/south. This intersection is a signalized intersection with four approaches.

Figure 3.2 displays the geometry of the intersection. SW Jefferson Ave consists of one lane in

each direction. The north approach along SW 9th St. consists of one lane in each direction. The

south approach along SW 9th St. consists of an exclusive right-turn lane and a through/left-turn

lane, separated by a bike lane.

Figure 3.1 Intersection of SW Jefferson Way and SW 9th Street (images obtained from Google
Maps)
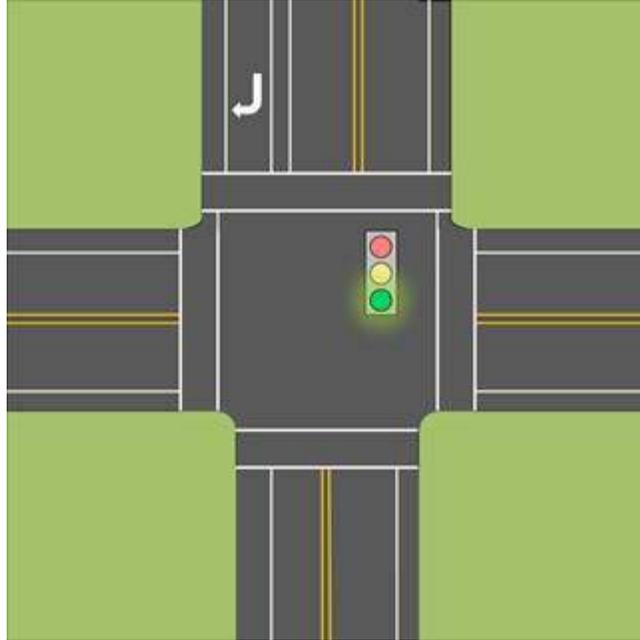
Figure 3.2 Intersection geometry

This intersection was selected for the SD investigation because it provides several obstructions to drivers attempting to maneuver through the intersection safely. A few examples of obstructions at this site include trees and shrubbery, utility poles and boxes, and placement of buildings. Furthermore, parked cars along the streets introduce another SD obstruction to drivers.

3.2 Lidar Data Acquisition and Processing

STLS lidar data were acquired at the intersection from nine independent set-ups strategically positioned throughout the scene. The scanner (Riegl VZ-400) was mounted to a wagon (figure 3.3) to increase efficiency. Each scan captured a 360-degree panorama of the scene, with a sampling resolution of 0.05 degrees. A Trimble R8 GNSS receiver was mounted to the top of the scanner to provide geodetic positioning. GNSS data were collected by using the Oregon Real Time GNSS Network (ORGN), which is managed by Oregon DOT.

To register scans together into a single model, 6–in. black and white checkerboard patterned targets were spread across the scene. The center points of these targets were captured by using a reflectorless total station sighted on the center of each target. These target centers were then linked to ground control points by positioning a 360-degree prism mounted on top of a rod placed on the ground control points. Geodetic coordinates for the ground control points were obtained from the ORGN. The registration process was completed with Leica Cyclone 9.0 software. In addition to utilizing the targets for the registration, cloud to cloud surface matching techniques were utilized to help improve the fit between overlapping scans. Figure 3.4 shows the point cloud consisting of the merged scans. It is colored by intensity values, which represent return signal strength. Note that this intensity information highlights highly reflective objects such as pavement markings.

The point cloud was edited to remove noise from passing vehicles and pedestrians since they were not static objects at the scene.

Figure 3.3 STLS mobile wagon set-up for stop-and-go scanning of the intersection.
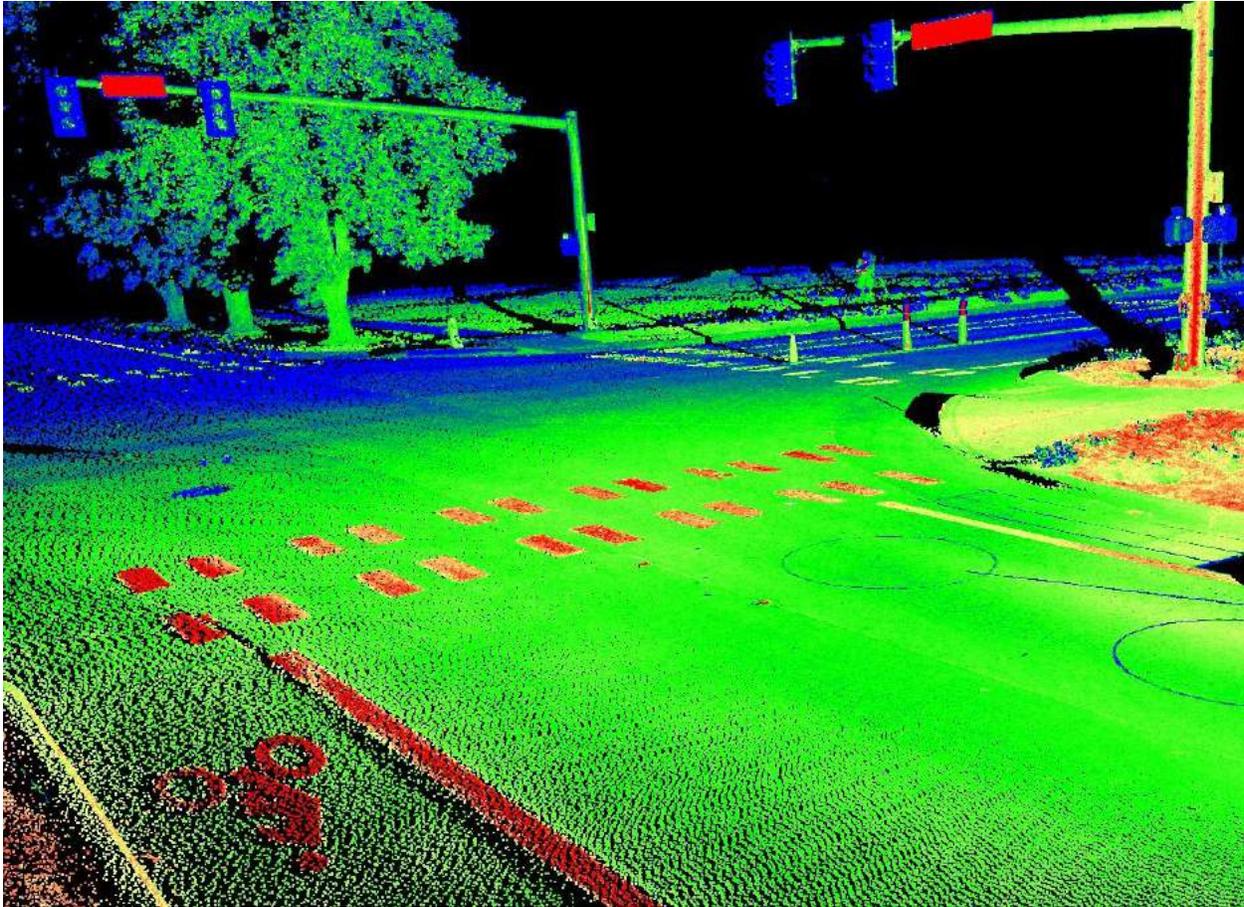
Figure 3.4 Combined point cloud colored by intensity, where red generally indicates highly reflective objects and blue represents less reflective objects.

3.3 SD Calculations and Reference Data Analysis

The ODOT procedure (Section 2.1.1) was followed to determine SD for the intersection of SW Jefferson Way and SW 9th Street. A full narrative of these activities is provided in Appendix A. Figure 3.4 shows a typical set-up during the field campaign.

Figure 3.5 Example SD study in progress

Chapter 4 Algorithm Development

<u>4.1 Driver Viewshed Algorithm</u>

An algorithm (SiDAL – Sight Distance Analysis using Lidar) was developed to detect

obstructions from the point cloud data (figure 4.1). The algorithm first organizes the point cloud

data into a 3D grid structure to generate 3D voxel representation of the road and surrounding

objects. Then, a line of sight analysis is performed to detect SD in a driver field of view and

determine where visibility is blocked. Finally, a driver viewshed map is generated. The

algorithms were developed and tested by using MATLAB and ArcMap software. The approach

was designed to be flexible such that one can vary the position of the driver as well as the level

of detail of the results. Each step will be discussed in more detail in this section.
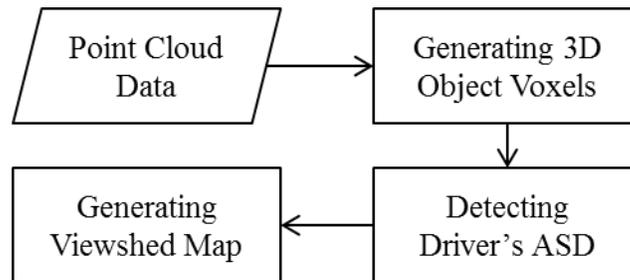
Figure 4.1 Algorithm flowchart

4.1.1 Generating a 3D Voxel Representation of Road Objects

A 3D voxel grid structure provides a simple representation of road objects captured in the

scans. For that purpose, the 3D space is first limited to user-defined distances from the driver

location along the x-, y-, and z-axis. Then, a user-defined grid size ($\square$) is used to divide the 3D

space into small, cubic volume pixels called voxels. The centroid location of each voxel is stored

in an index matrix for fast recall. Voxels containing more than a predefined number of scan

points are identified as object voxels, and their indices are stored separately. These object voxels

code obstructions versus visible space and were further used in the line of sight analysis. A sample point cloud captured of a tree and the tree with its corresponding object voxels developed by this algorithm are shown, respectively, in figure 4.2 (a) and (b).
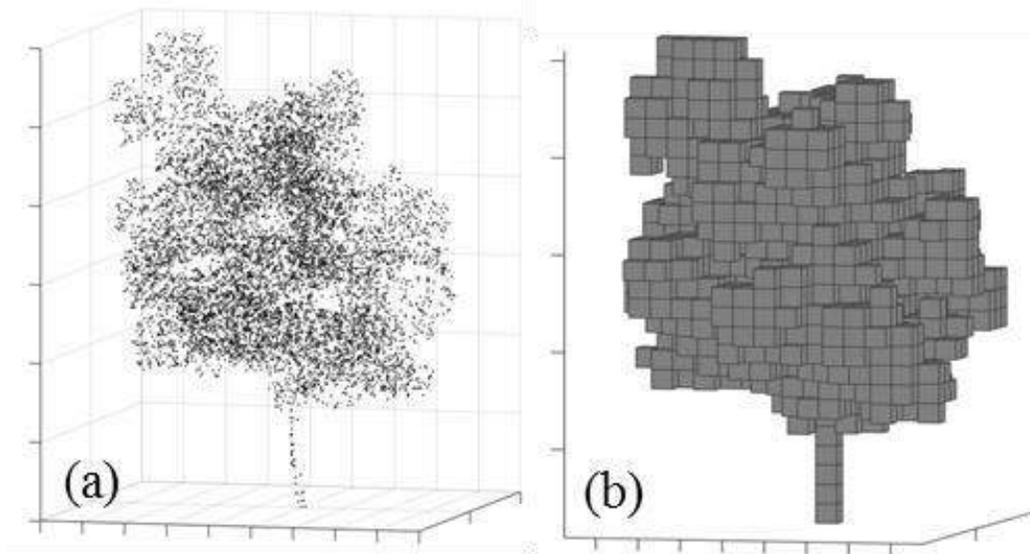
Figure 4.2 (a) Point cloud and (b) 3D voxel representation of a tree

A suitable voxel grid size that is greater than the typical point spacing in the point cloud should be selected. Finer grids generally result in more realistic representation of objects and thus a more accurate driver viewshed, since they can account for smaller objects. However, selecting a small grid size may also cause higher computational costs, i.e., processing time. Therefore, an optimal parameter set should be chosen, which will be explored in Section 5.1.

4.1.2 Detecting Driver's ASD

The driver's lines of sight are generated and used to determine areas visible to the driver within a 2D slice of the data. Figure 4.3 illustrates a schematic 2D projection of the driver location, lines of sights, and an obstruction (figure 4.3 (a)) as well as their voxel representation (figure 4.3 (b)). Lines of sight start from the driver location and extend as rays along different

directions defined by an angular resolution. The angular resolution is defined as a spacing *a* at a distance *r* from the driver.

Line of sight voxels within the 3D grid space developed in the previous step are recognized by using the Bresenham's algorithm (Joy 1999), which identifies cells within a grid that formulate an approximation of a straight line. The indices of these designated voxels for each line are stored. Having the object and lines of sight voxels, obstructions (shown in red in figure 4.3) and visible areas (shown in green in figure 4.3.) can be determined.
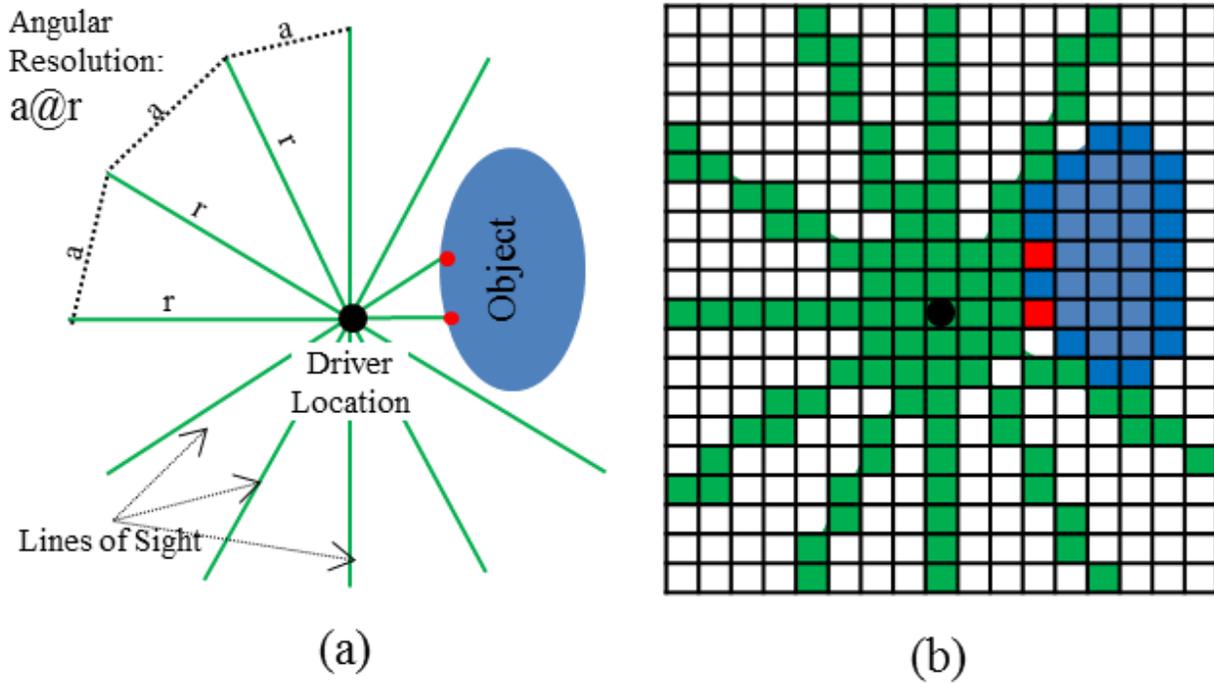
Figure 4.3 (a) Schematic showing the 2D projection of a driver's line of sight and an obstruction object and (b) Voxelized representation of object and lines of sight

A fine angular resolution (i.e., the smaller "a" distance shown in figure 4.3) results in more accurate obstruction detection. However, increasing the number of lines of sight in the analysis increases computational complexity. Too low of an angular resolution (large a) can

31

cause arbitrary void spaces in the detected visible areas (figure 4.3a). Therefore, similar to the grid size, an optimum angular resolution should be chosen (see Section 5.1).

4.1.3 Generating a Viewshed Map

Finally, the binary raster map that identifies locales as visible or not is exported to ArcMap. The binary raster can be converted to a polygon for simplification. This process is completed by importing a point (centroid) for each raster cell that is visible and then converting those combined points into a single polygon that bounds those points.

4.2 Algorithm Performance Evaluations

Tests were conducted to evaluate the performance and accuracy of the SiDAL algorithm in considering several combinations of input parameters by using the workflow shown in figure 4.4. To represent ground-truth, a viewshed polygon was manually generated from the point cloud. The algorithm and the lidar point cloud data were used to generate viewshed polygons for a driver at specific location for each parameter set. The process was repeated hundreds of times using different voxel grid sizes and angular resolutions in order to observe their impact on the algorithm runtime and accuracy of results.
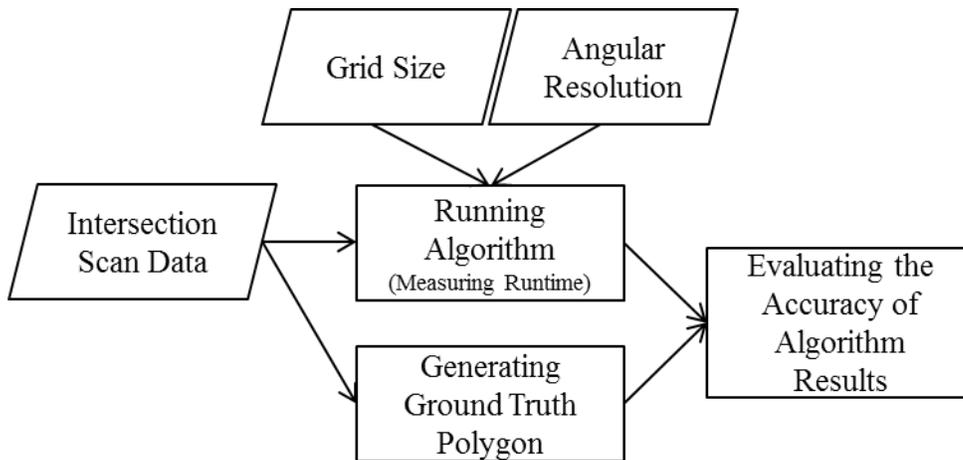
Figure 4.4 Evaluation flowchart

4.2.1 Generating a Ground Truth Viewshed Polygon

A viewshed polygon was manually generated in the ArcMap environment and used as a ground truth in the evaluations. As horizontal lines of sight were used in the tests, obstructions in the driver's horizontal lines of sight were identified for the test. The cut-plane tool in the Leica Cyclone software was used to create a slice of point cloud data within a one meter range at the driver height. Points from noise (e.g., passing cars) were removed so that only the points which represented static objects that might obstruct horizontal lines of sight were kept. Figure 4.5 (a) shows the whole point cloud data set for the intersection, while figure 4.5 (b) presents the isolated points in the horizontal slice. Then, the isolated points were exported and imported into ArcMap where they could be used to manually draw a polygon representing the driver viewshed. Figure 4.5 (c) presents the exported isolated points (obstruction points), driver location, and the ground truth viewshed polygon in a GIS map.
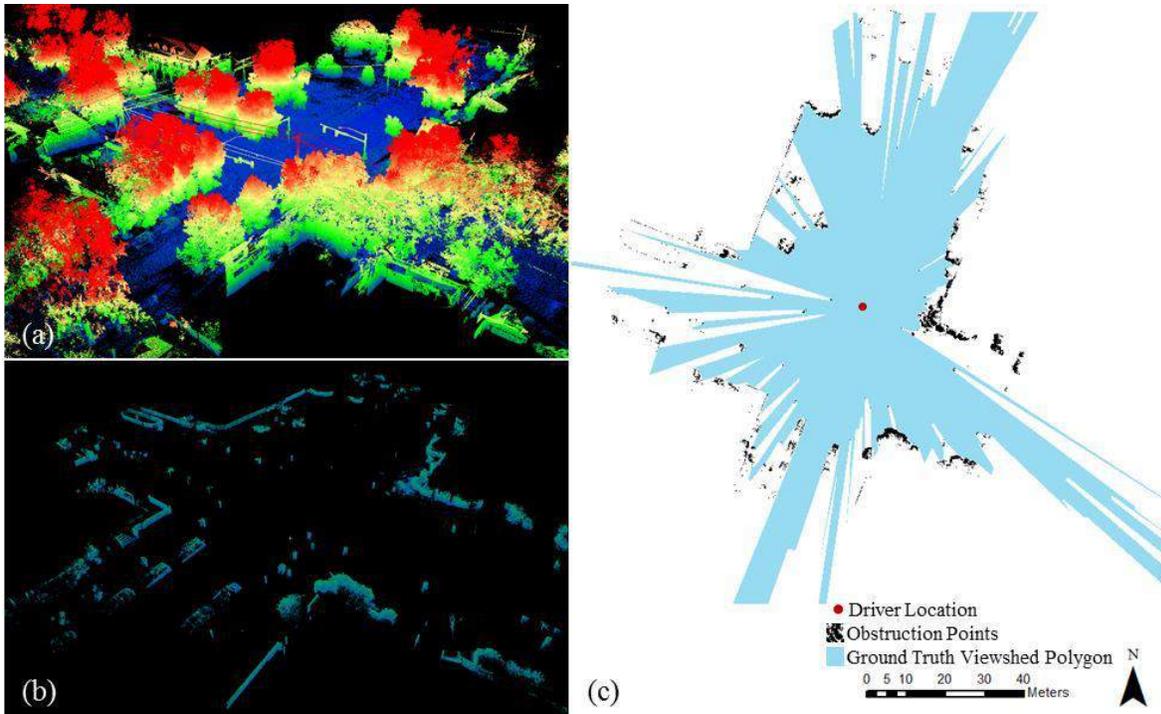
Figure 4.5 Evaluation flowchart showing (a) full point cloud, (b) cross section through the data set, and (c) ground truth polygon digitized from the obstructions.

4.2.2 Evaluating the Accuracy of Results

To evaluate the accuracy of the SiDAL algorithm result employing different grid sizes and angular resolution combinations, algorithm-generated polygons were compared with the ground truth polygon. For this analysis, the data were cropped to the roadway, and the differences in visible surface area were calculated for the comparison.

Two types of false detection can happen: false positives and false negatives (figure 4.6). On the one hand, the false positive is an area in the result polygon that is not included in the ground truth polygon. These are locations where the algorithm over-predicts visibility. On the other hand, a false negative is an area in the ground truth polygon that is not included in the result polygon. These are locations where the algorithm under-predicts visibility.

34
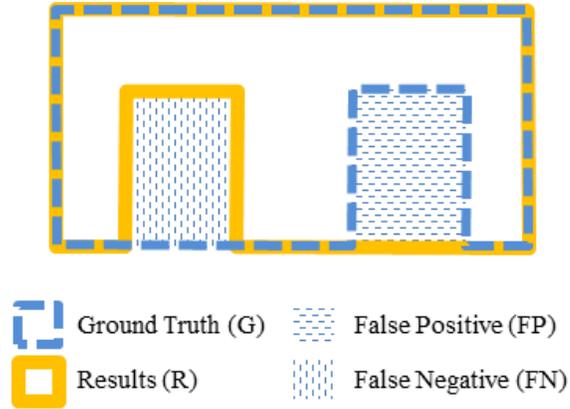
Figure 4.6 Schematic illustration of errors

Equations 4.1 and 4.5 present how the percentage of error was calculated after each run of the algorithm considering both false positives and false negatives:

$$Error_{area} = FP_{area} + FN_{area} = (G \cup R)_a - (G \cap R)_{area} \qquad \text{Equation 4.1}$$

$$Er(\%) = \frac{Error_{area}}{G_{area}} \qquad \text{Equation 4.2}$$

where: FP is false positive, FN is false negative, G is the ground truth polygon, and R is the algorithm result polygon.

4.4. Analysis of the Impact of Driver Height and Type of the Vehicle on SD

The flexibility of the SiDAL algorithm enables one to evaluate the visibility of different driver heights and vehicles. Also, the vehicle can be positioned in any lane, enabling one to evaluate several different types of potential traffic motions. Another advantage is that one can consider multi-modal forms of transportation such as pedestrians and bikes. A few common scenarios were evaluated in this pilot project by varying the position and height of the driver.

4.5 Virtual Reality Assessments

     The GeoMat VR (Virtual Reality, figure 4.7) system in the Civil and Construction Engineering Geomatics Research Lab at OSU was utilized as another mechanism to validate the results of the algorithm. Full details of this system were provided by O'Banion (2016), and it was built following a hardware configuration developed by Dr. Oliver Kreylos (University of California, Davis). This immersive VR system consists of a Samsung 65inch active 3D LED television, 3D stereoscopic glasses, an Optitrack™ infrared motion capture system, and a Nintendo Wii controller. Three Optitrack™ cameras monitor tracking antlers mounted on the user's stereoscopic glasses and Wii controller. The VR software platform used is the *VRUI 3.1* (Virtual Reality User Interface), which contains an open-source software module for visualizing point cloud data called *LidarViewer 2.12,* which runs in the Unix environment. A separate computer with the MS Windows OS runs the Optitrack™ motive software. The system enables a high level of visualization and interaction with digital, 3D data such as lidar point clouds.

     In this study the base point cloud for the intersection was imported as well as the viewshed output from SiDAL. In GeoMAT VR, users are able to quickly reposition themselves throughout the scene. Hence, they can place themselves at the point of view where the viewshed was generated, but then move out of that view to further evaluate the obstructions and influence of those obstructions on the viewshed. This flexibility was very helpful for evaluating the algorithm's effectiveness in detecting obstructions.

Note: Stereoscopic visualization was disabled for the purpose of acquiring these photographs.

Figure 4.7 Overview image of GeoMat VR, including IR tracking cameras (left) and an example of a user interacting with the system (right) (from O'Banion 2015).

Chapter 5 Results

5.1 Algorithm Performance Evaluations

5.1.1. Computation Time

The impact of voxel grid size ($\square$) and angular resolution on SiDAL algorithm runtime

was investigated. In the first test, the algorithm was run with equal grid size and angular

resolution. As shown in figure 5.1 (a), the test indicated that the runtime increases when finer

grid sizes and angular resolutions are used. However, the increase in the runtime is very

significant for grid sizes smaller than 0.5 meters. Even though the runtime is less than 100

seconds for all grid sizes greater than 0.5 meters, it jumps up to approximately 70,000 seconds

for grid sizes equal to 0.2 meters. In the second test, the algorithm was run with different angular

resolutions than the grid size. Figure 5.1 (b) shows that the runtime increases when a finer

angular resolution is chosen (even when the grid size is kept consistent); however, the impact of

angular resolution on runtime is not as significant as the impact of changing the grid size.
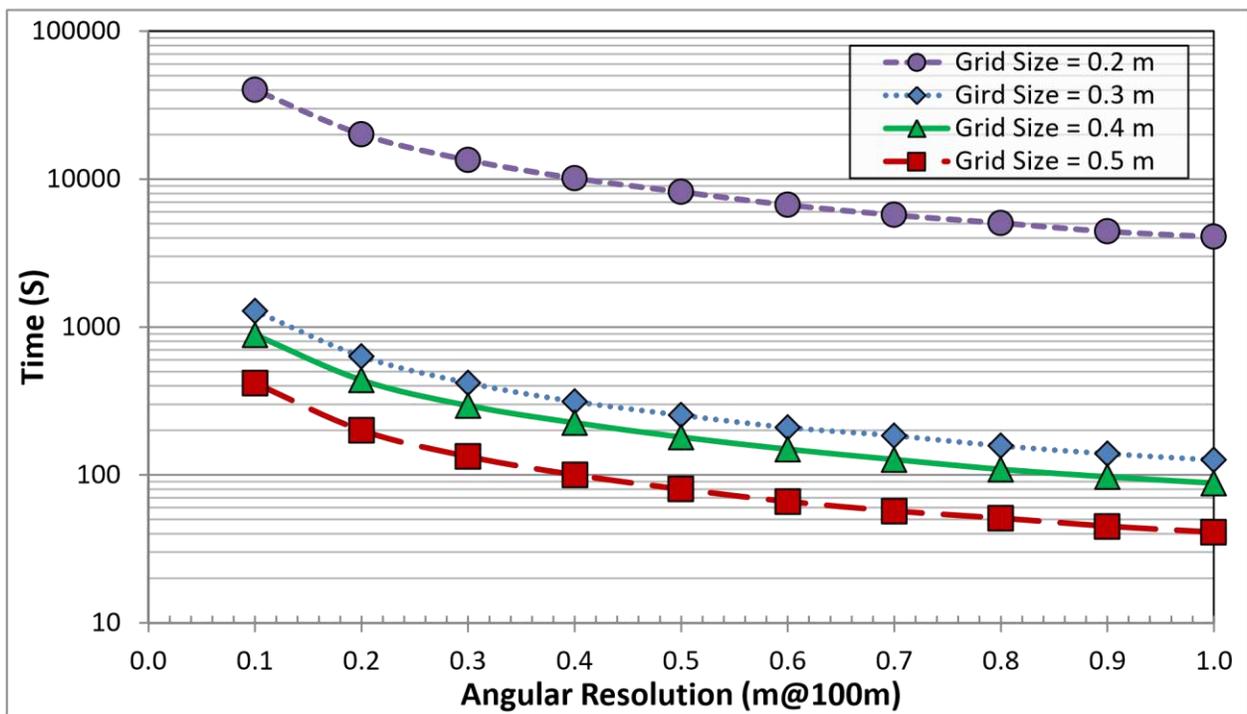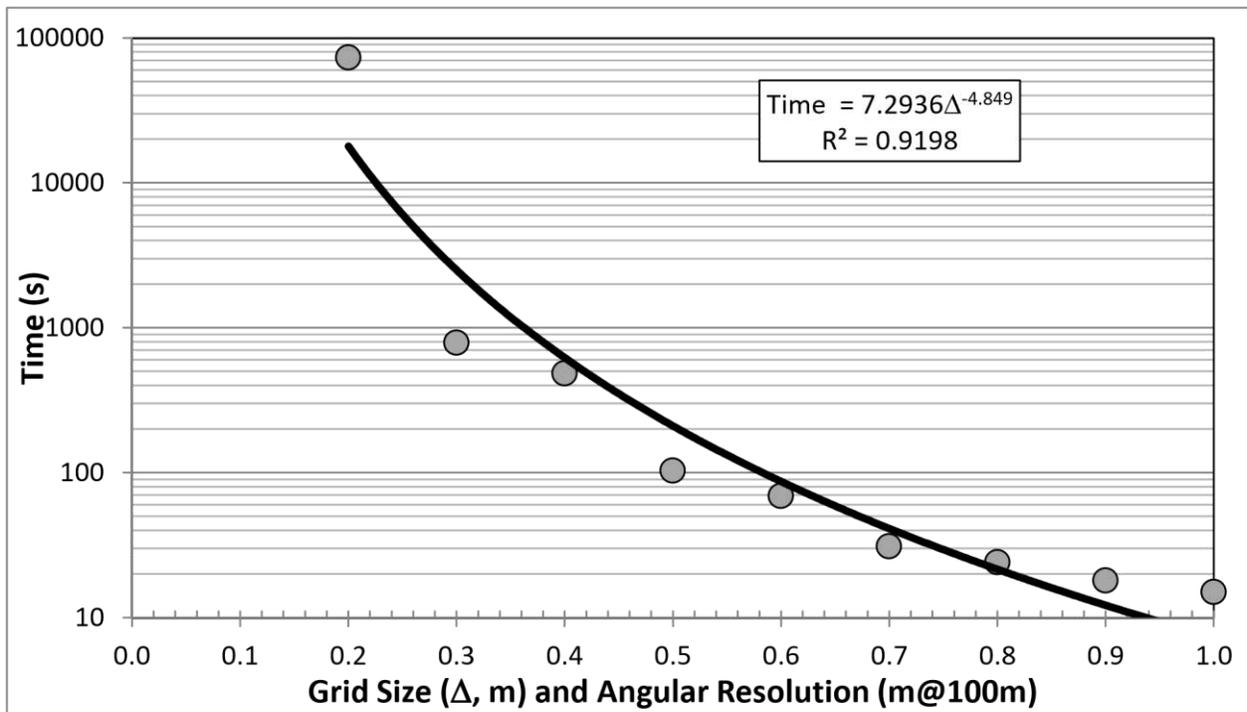
Figure 5.1 Algorithm runtime for (a) equivalent and (b) varying grid size and angular resolution

5.1.2 Algorithm Accuracy Evaluation

The influence of grid size and angular resolution on the accuracy of algorithm visibility detection results was also evaluated. Similar to the runtime evaluation process, the algorithm was first run with equal grid size and angular resolution values. As shown in figure 5.2 (a), the test indicated that the accuracy of results increases with finer grid sizes and angular resolutions. However, although the percentage of error drops significantly (from 15percent to 6 percent) when the grid size changes from 1.0 to 0.6 meters, the change in error percentage is very minor for grid sizes smaller than 0.6 (i.e., the error remains around 5 percent).

In the second test, the algorithm was run with different angular resolution and grid size combinations. Figure 5.2 (b) presents the impact of angular resolution on the algorithm accuracy as well as its correlation with the grid size. As shown in figure 5.2 (b), the test indicated that if angular resolution is selected from values equal to or greater than the grid size but smaller than 1.5 times the grid size, the error will be less than 6 percent. However, choosing angular resolution outside of this range can result in higher percentages of error. An angular resolution finer than the grid size can cause over-sampling, which generates error in the line of sight analysis. Finally, an angular resolution greater than 1.5 times the grid size will cause arbitrary void spaces in the detected visible areas, thus resulting in higher error percentages.
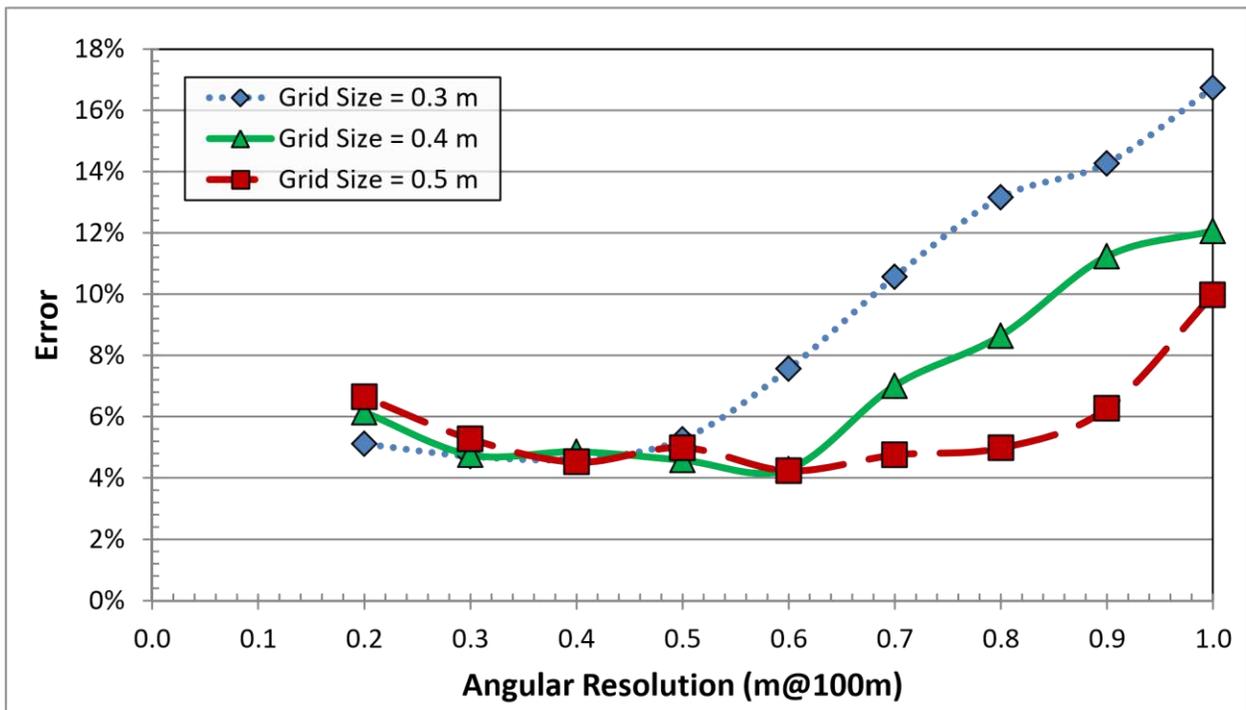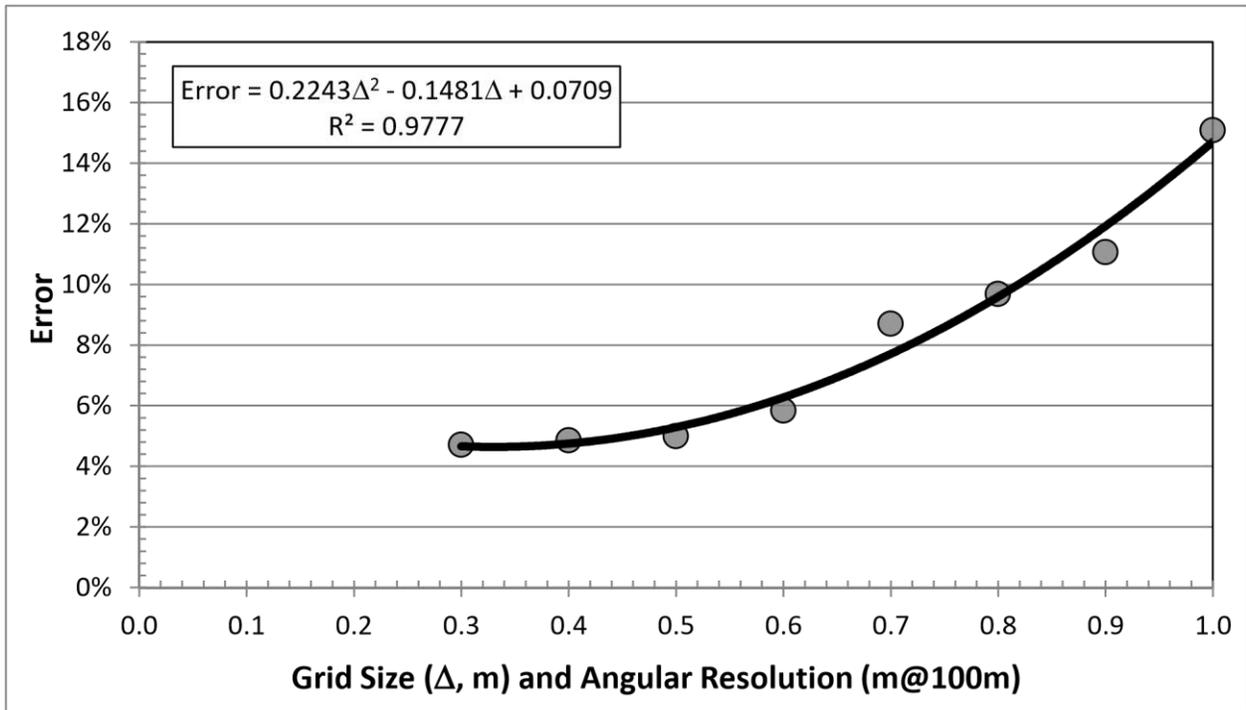
Figure 5.2 Algorithm error percentage for (a) equivalent and (b) varying grid size and angular resolution

5.2 Conventional Analysis

Table 5.1 provides the SD analysis summary for the study conducted at SW Jefferson Way and SW 9th Street. The required SSD and ISD measurements were based on the requirements provided by AASHTO for a design speed of 25 mph (AASHTO 2011). The measurement used for the ISD for each approach was the smallest distance measured to the right following AASHTO recommendations. The smallest measurement was used for comparison to be conservative and to guarantee the safety of the intersection. Furthermore, AASTHO (2011) states "if the available [ISD] for an entering or crossing vehicle is at least equal to the appropriate [SSD] for the major road, then drivers have sufficient [SD] to anticipate and avoid collisions." This is the case for all ISD measurements when they are compared to the required and calculated SSD. However, this is not the case when they are compared with the measured SSD. On the basis of the data collected, the intersection had sufficient SSD and ISD for nearly all approaches; however, the eastbound approach did not provide adequate ISD and would require mitigation of the intersection obstructions to meet the requirements for ISD.

Table 5.1 SW Jefferson Way at SW 9th Street SD analysis summary

Approach	Stopping Sight Distance (ft)			Intersection Sight Distance (ft)		
	Required	Calculated	Measured	Required	Calculated	Measured
Northbound	155	151.86	279	275.6	275.63	294
Southbound	155	151.86	681	275.6	275.63	330
Eastbound	155	151.86	633	275.6	275.63	217
Westbound	155	151.86	681	275.6	275.63	459

5.2 Comparison of the SiDAL Algorithm with the Conventional Approach

Conventional sight distance triangles were generated from the traditional field measurements. These measurements were then visually compared to the results from the SiDAL algorithm for each approach (figure 5-3).
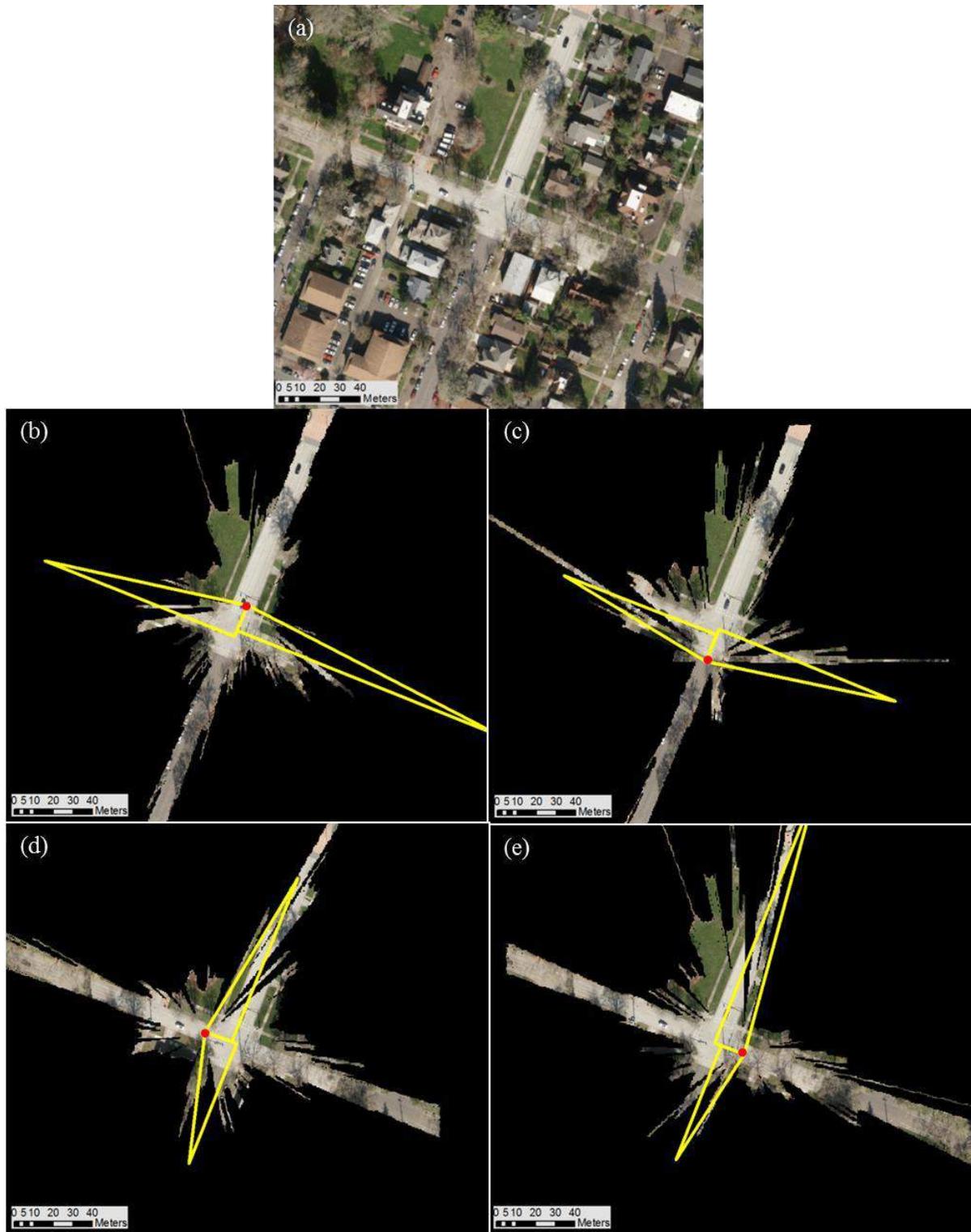
Figure 5.3 Stopping sight distance triangles overlain on the visible scene determined with theSiDAL algorithm for the Jefferson intersection evaluating each traffic approach (a) North, (b) South, (c) West, (d) East.

5.3 Analysis of the Impact of Driver Height and Type of the Vehicle on SD

In addition to evaluating each approach, several potential scenarios were also analyzed. One example was varying the driver height, which can influence the extent of visible roadway (figure 5.4). Another example was the differences in visibility depending on the position of the vehicle for traffic movements, as well as considering a bicyclist's visibility at the intersection (figure 5.5).
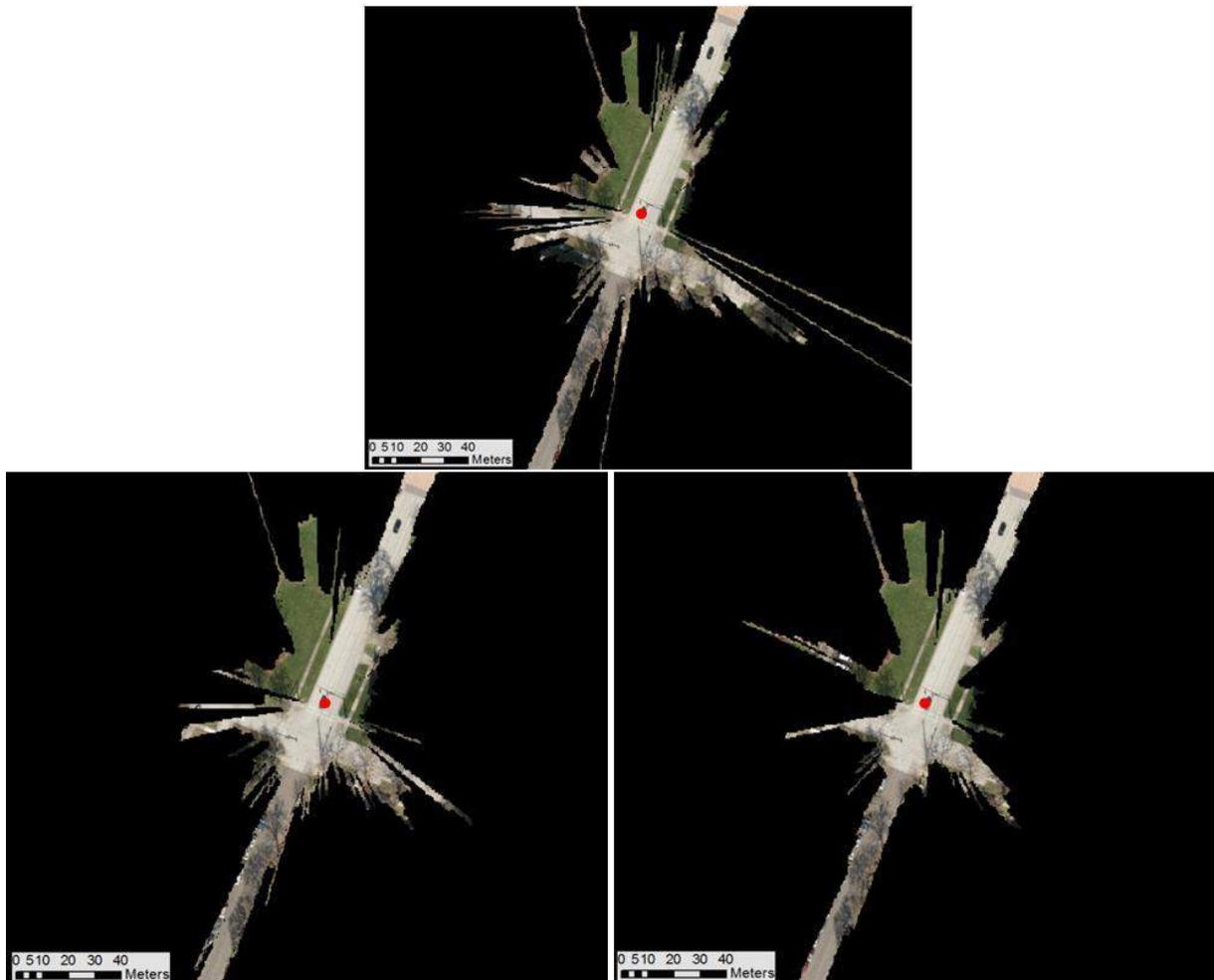
Figure 5.4 Differences in visibility determined with the SiDAL algorithm using varying driver heights
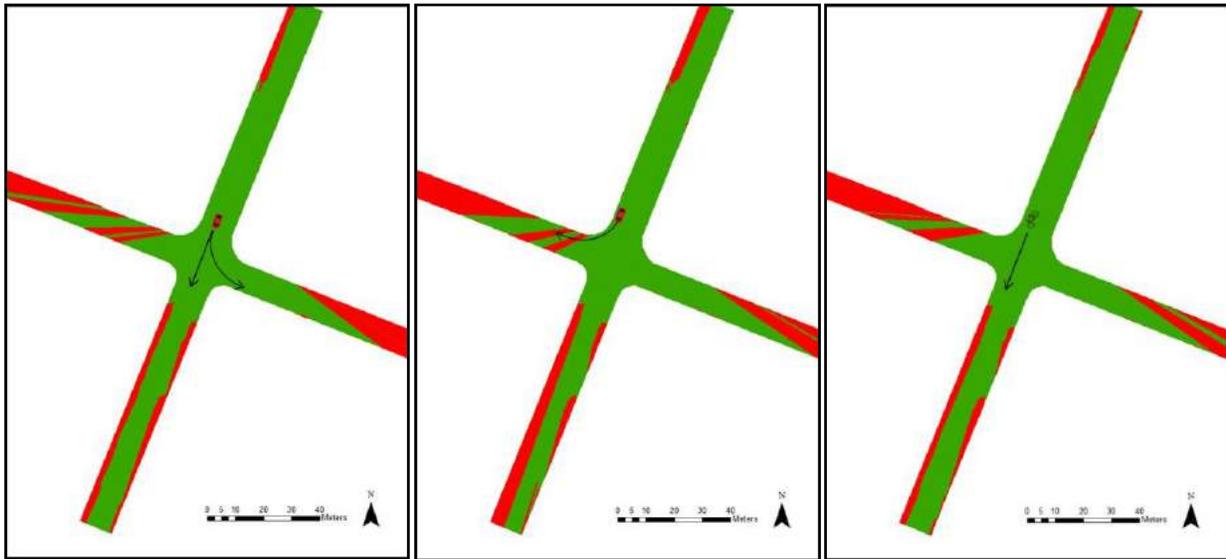
Figure 5.5 Example visibility differences for (a) vehicle positioned to proceed straight through an intersection or to perform a left turn, (b) a vehicle poised for a right hand turn, and (c) a bicyclist proceeding straight through the intersection

5.4 Virtual Reality Assessments

Figures 5.6 through 5.8 show examples of the visibility assessment in the GeoMAT VR. Viewshed outputs from SiDAL were imported and visually validated with the point cloud. In this example (figure 5.7), the green points represent the viewshed and can be seen to terminate when intersecting objects such as a pole. In this immersive environment, users can quickly put themselves into the position of where the viewshed is generated and pull themselves out to evaluate each obstruction and its influence on the viewshed (figure 5.8).

(a)

(b)

Figure 5.6 Point cloud scene viewed in virtual environment from (a) third person view and (b) first person view

Figure 5.7 An example of a visibility analysis conducted in the GeoMAT CAVE. The blue shaded point cloud represents the objects present in the scene. The green dots represent the 2D viewshed.
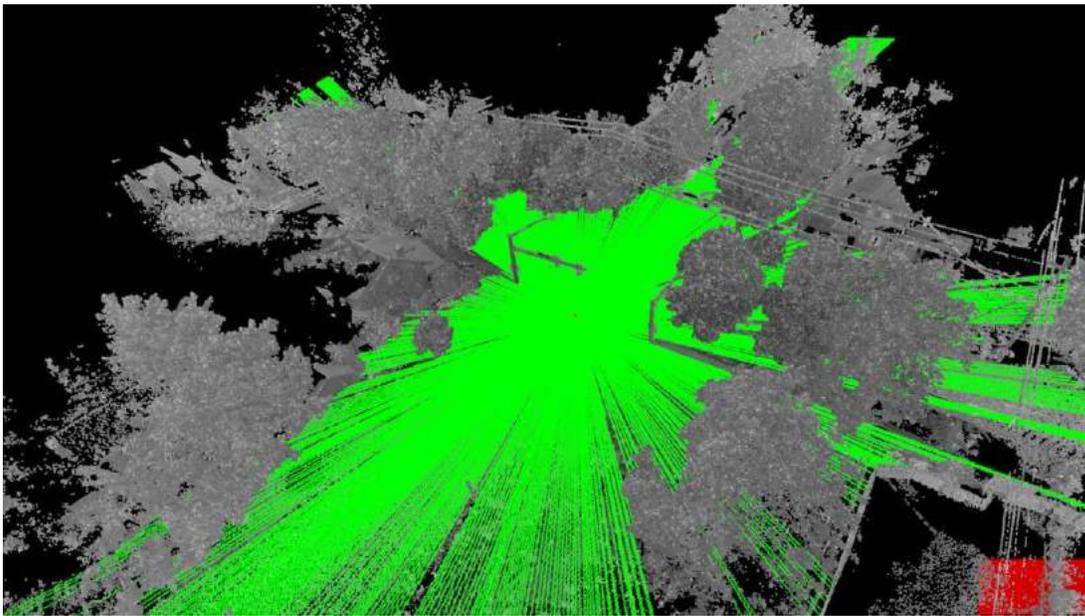
Figure 5.8 Alternative view of the data in figure 5-5 showing the termination of the viewshed with the point cloud

Chapter 6 Discussion

6.1 Algorithm Performance Evaluations

The algorithm performance evaluations indicated that an optimum grid size equal to 0.5 meters combined with an angular resolution equal to 0.5 meters at a 100-meter range result in reasonable runtime (approximately 60 seconds) and accuracy (approximately 5 percent error). A finer grid size could also be used, but as shown in figures 5.1 and 5.2, the amount of accuracy improvement will be relatively minor and likely not worth the significant increase in the required algorithm runtime. This optimum algorithm setting was used in the other steps of this research.

6.2 Comparison of the SiDAL Algorithm with the Conventional Approach

The SiDAL algorithm showed significantly more detail in comparison to the conventional results. In addition, because of the few discrete measurements made in the conventional approach, the conventional approach significantly over predicts visible areas in the road that could be important to a driver's response. For example, in figure 5.2, the sight triangles for each site have major gaps where the SiDAL algorithm indicated that an obstruction would block someone's view.

6.3 Analysis of the Impact of Driver Height and Type of the Vehicle on SD

In the analysis of driver height (figure 5.3), the visibility was shown to change significantly based on driver height or vehicle type. The algorithm also provides flexibility to evaluate visibility for multi-modal transportation (e.g., figure 5.4c), which is not well reflected in the conventional approach. A key advantage of the SiDAL algorithm is it provides the ability to evaluate multiple scenarios so that the most significant obstructions can be remedied.

Although the case study intersection represented a very simple intersection, the advantage to the SiDAL approach is that it can handle much more complex intersections, provided that the appropriate lidar survey data can be obtained.

49

Chapter 7 Conclusions and Recommendations

In this research, an algorithm (SiDAL) was developed to perform 3D sight analysis using lidar data. This algorithm simplifies the data into a voxelized form and then enables users to evaluate visibility from a variety of perspectives throughout the scene. This flexibility enables the algorithm to successfully evaluate sight distance constraints from a variety of vehicles and driver heights as well as multi-modal forms of transportation. The algorithm can handle complex objects throughout the scene and showed several benefits over conventional measurements. First, data can be collected safely from the side of the road. Second, more details about the road and obstructions are collected and can be considered. Third, it provides more flexilbility in evaluating various modes of transportation, including multi-modal transportation, which is becoming increasingly important for reducing congestion in urban areas and promoting public health. Finally, the conventional approach significantly over-estimated the visible portion of the intersection, which can lead to unsafe intersections that do not provide adequate sight distance being considered safe.

7.1 Technology Transfer

In addition to dissemination of this final report through PacTrans, resources will be made available on the website http://learnmobilelidar.com, which has international visibility. Multiple presentations focused on the results of this research project at the following venues:

- Pactrans Annual Meeting (October 2015, Seattle, Wash.)

- Northwest Transportation Conference (March 2015, Corvallis, Ore.)

- University of Utah (March 2016, Salt Lake City, Utah)

- California State Polytechnic, Pomona (March 2016, Pomona, Calif.)

- International Conference on Sustainability in Design, Engineering, and Construction (ISCDEC, April 2016, Phoenix, Ariz.).

- Pactrans Annual Meeting (October 2016, Seattle, Wash.)

7.2 Future Research

Several avenues of future research were identified in expanding this algorithm.

- ➢ Multi-modal – continue to evaluate a broad range of vehicle types and modes of transportation (e.g., bikes, pedestrians) and adapt for specific visibility constraints.

- ➢ Kinematic SD analyses – The SiDAL algorithm can easily be scripted to show visibility at multiple time steps as a vehicle or bike moves through the scene.

- ➢ Insertion of objects – 3D objects could be placed within the viewshed to model proposed signs or structures, construction equipment, or other obstructions.

- ➢ Narrow the field of view to account for typical ranges of motion of where drivers will actually be looking.

- ➢ Further integration with VR technology (e.g., CAVE and Driving Simulator)– While this study initially explored the use of 3D technology to validate the results, there are many potential paths of exploration. For instance, eye-tracking can be implemented to determine where someone is looking in 3D space. Objects that are viewed by a person at specific viewpoints could be tracked, thus enabling missed objects to be identified.   Head mounted displays could also potentially offer a more realistic assessment and be used to digitally paint the scene of what a user can see as they progress forward with traffic motions. Ultimately, this could be a powerful tool for validating 3D design alternatives and mitigating issues early in the design process.

- ➢ The SiDAL algorithm would be straightforward to apply to other forms of SD (e.g., curves, both horizontal and vertical).

References

AASHTO. (2001). *A Policy on Geometric Design of Highways and Streets*.

AASHTO. (2011). *A Policy on Geometric Design of Highways and Streets*.

Arizona DOT. (2013). Chapter 11 Highway Design. In *Highway Design*.

Caltrans. (2001). "Chapter 500 Traffic Interchanges." *Highway Design Manual*.

Caltrans. (2006). Chapter 1000 Bikeway Planning and Design. In *Highway Design Manual*.

Caltrans. (2014a). "Chapter 400 Intersections at Grade." *Highway Design Manual*.

Caltrans. (2014b). "Chapter 200 Geometric Design and Structure Standards." *Highway Design Manual*.

Castro et al. (2011)

Castro et al. (2014)

Castro et al. (2015)

Chen, A., Golparvar-Fard, M., and Kleiner, B. (2013). "Design and Development of SAVES: A Construction Safety Training Augmented Virtuality Environment for Hazard Recognition and Severity Identification." *Journal of Computing in Civil Engineering*, 841-848.

Colorado DOT. (2011). Chapter 14 Bicycle and Pedestrian Facilities. In *Roadway Design Guide*.

Dickinson, J. K., Woodard, P., Canas, R., Ahamed, S., and Lockston, D. (2011). "Game based trench safety education: development and lessons learned." Journal of Information Technology in Construction, 16, 119-133.

Fambro, D., Fitzpatrick, K., and Russell, C. (2007). "Operating Speed on Crest Vertical Curves with Limited Stopping Sight Distance." *Transportation Research Record: Journal of the Transportation Research Board*, Transportation Research Board of the National Academies.

Federal Highway Administration." (n.d.). "Speed Concepts: Informational Guide."

Fitzpatrick, K. (2003). *Design Speed, Operating Speed, and Posted Speed Practices, Issue 504, Part 1*. Transportation Research Board.

Guo, H., Li, H., Chan, G., and Skitmore, M. (2012). "Using game technologies to improve the safety of construction plant operations." *Accident Analysis and Prevention*, 48, 204-213.

Hall, n.d.).

Hassan, Y., Easa, S. M., & El Halim, A. O. A. (1996). Analytical model for sight distance analysis on three-dimensional highway alignments. Transportation Research Record: Journal of the Transportation Research Board, 1523(1), 1-10.

Hinze, J. W., & Teizer, J. (2011). Visibility-related fatalities related to construction equipment. Safety science, 49(5), 709-718.

Iowa DOT. (2015). Chapter 6 Geometric Design Sight Distance. In *Design Manual*.

Ismail and Sayed 2007

ITD. (2007). *Existing Conditions - Roadways*.

ITD. (n.d.). *Practical Solutions for Highway Design*.

Jha and Karri 2009

Jha et al. 2011

Joy, K. I. (1999). Breshenham's algorithm. Visualization and Graphics Research Group, Department of Computer Science, University of California, Davis.

Khattak, A. J., & Shamayleh, H. (2005). Highway safety assessment through geographic information system-based data visualization. Journal of computing in civil engineering, 19(4), 407-411.

Khattak, A. J., Hallmark, S., & Souleyrette, R. (2003). Application of light detection and ranging technology to highway safety. Transportation Research Record: Journal of the Transportation Research Board, 1836(1), 7-15.

Khattak, A., & Gopalakrishna, M. (2003). Remote Sensing (LIDAR) for Management of Highway Assets for Safety (No. MTC Project 2001-02,).

Layton, R., and Dixon, K. (2012). "Stopping Sight Distance." *The Kiewit Center for Infastructure and Transportation*, (April).

Lin, K. Y., Son, J. W., and Rojas, E. M. (2011). "A pilot study of a 3D game environment for construction safety education." *Journal of Information Technology in Construction*, 16, 69-83

McKinley, L. (2011). "Sight Distance." *Oregon Department of Transportation*.

McKinley, L. (2014). "Sight Distance Standards and Deviations for Highway Approaches." *Oregon Department of Transportation*.

MnDOT. (2007). Chapter 5: Share-Use Paths. In *Mn/DOT Bikeway Facility Design Manual*.

Namala, S. R., & Rys, M. J. (2006). Automated calculation of passing sight distance using global positioning system data (No. K-TRAN: KSU-03-2). Kansas Department of Transportation.

O'Banion 2015

O'Banion (2016

Olsen et al. 2013

Oregon DOT. (2012). "Chapter 3 Elements of Design." *Highway Design Manual*.

Park, C. S., and Kim, H. J. (2013). "A framework for construction safety management and visualization system." Automation in Construction.33, 95-103.

Santos & Castro (2014)

Shamayleh, H., & Khattak, A. (2003). Utilization of LiDAR technology for highway inventory. In Proc. of the 2003 Mid-Continent Transportation Research Symposium, Ames, Iowa.

Smith, D., & McIntyre, J. (2002). Handbook of Simplified Practice for Traffic Studies (No. Iowa DOT Project TR-455,).
http://www.ctre.iastate.edu/pubs/traffichandbook/4SightDistance.pdf

Squelch, A. (2001). "Virtual Reality for Mine Safety Training in South Africa." The Journalof the South African Institute of Mining and Metallurgy. 209-216.

Texas DOT. (2014). *Roadway Design Manual*.

Transportation Research Institute. (1997a). "Stopping Sight Distance and Decision Sight Distance." *Oregon State University*.

Transportation Research Institute. (1997b). "Intersection Sight Distance." *Oregon State University*.

Tsai, Y., Yang, Q., & Wu, Y. (2011). Use of Light Detection and Ranging Data to Identify and Quantify Intersection Obstruction and Its Severity. Transportation Research Record: Journal of the Transportation Research Board, 2241(1), 99-108

Wisconsin DOT. (2013a). Chapter 1260 Sight Distance. *WSDOT Design Manual*.

Wisconsin DOT. (2013b). Chapter 1310 Intersections. In *WSDOT Design Manual*.

Yan, X., Radwan, E., Zhang, F., & Parker, J. C. (2008). Evaluation of Dynamic Passing Sight Distance Problem Using a Finite-Element Model. Journal of Transportation Engineering, 134(6), 225-235.

Zhao D., Lucas, J. and Thabet, W. (2009). "Using virtual environments to support electrical safety awareness in construction." In Proceedings of the 2009 Winter Simulation Conference, Austin, Texas. 2679-2690.

Appendix A: Sight Distance Analysis for SW Jefferson Ave and SW 9th St

<u>A.1 Procedure for Measuring SD</u>

The ODOT procedure (Section 1.1.1) was followed to determine SD for the

intersection of SW Jefferson Way and SW 9th Street. An object 2 feet in height was placed at

the centerline, 19 feet away from the stop line, representing the average vehicle length

(AASHTO, 2011). From there, the person walked away from the stop line using a measuring

wheel to measure the distance until the object was no longer visible or until it was unsafe for

the data collector to continue. A sighting height of 3.5 feet is used based on the driver's

height. This procedure was repeated for each approach.

When measuring the ISD at the intersection of SW Jefferson Way and SW 9th Street the

procedure posted by ODOT was used. To measure ISD in the field, ODOT posted a *Technical*

Services Bulletin that describes the procedure to measure SD at intersections with a stop control

at the approach (McKinley 2014). There are four steps in the procedure, beginning with

recording the number of lanes on the highway and their widths (McKinley 2014). The next steps

include measuring the roadway grades with a Smartlevel at the steepest section within 900 to

1,500 feet left and right of the intersection and recording the posted speed (McKinley 2014). For

the intersection of SW Jefferson Way and SW 9th Street, the grade was minimal and therefore not

recorded. The final step is to measure the SD. To do this, four objects must be set up in line with

the center of the proposed intersection (McKinley 2014). Object 1 is located opposite of the fog

stripe/curb at a height of 2.0 feet (McKinley 2014). The second object is located near the fog

stripe/curb also at a height of 2.0 feet (McKinley 2014). The third and fourth objects are located

behind the near fog stripe/curb at heights of 3.5 feet (McKinley 2014). A sighting height of 3.5

feet is used based on the driver's height. Figure A.1 shows the placement of each object and a

detailed diagram of the procedure. This diagram can be found in ODOT's procedure for

measuring SD at intersections with a stop control at the approach.
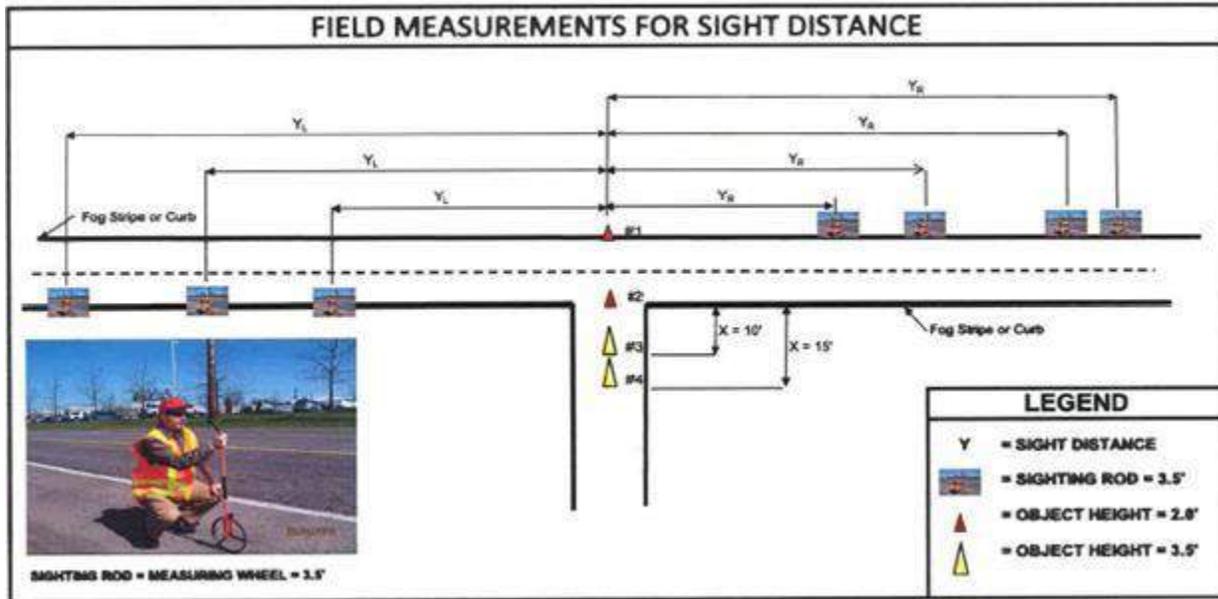
Figure A.1 SD measurement procedure diagram (McKinley 2014)

All the measurements from the left are taken from the near fog stripe/curb, while all the

measurements from the right are taken from the opposite fog stripe/curb (McKinley 2014).

Starting on or near the fog stripe/curb and at the centerline of the approach, set the measuring

wheel to 0 feet and walk along the roadway until you cannot see any of the markers (McKinley

2014). From there the distance is recorded. This process is continued for the remaining markers

or until the maximum distance of 900 to 1500 feet is reached (McKinley 2014). For this study

the maximum distance was never reached. The measurements from right of the approach are to

objects 1, 2, 3, and 4. Measurements taken from the left of the approach are to objects 2, 3, and 4

(McKinley 2014). The sight triangle is clear of obstructions if the distance measured from the

objects is 900 to 1500 feet or more (McKinley 2014). Figure A.2 shows an image of the study taking place.

A.2 Calculation of SSD and ISD

For all approaches at SW Jefferson Way and SW 9th Street, the posted speed was 25 mph. For the SSD and ISD calculations the posted speed was used, assuming that the design speed and the posted speed were the same. The deceleration rate used for the SSD calculation was the AASHTO recommended rate (3.4 m/s^2, 11.2 ft/s^2). The calculated SSD for the intersection of SW Jefferson Way and SW 9th Street was 46.53 meters (151.86 feet).

For calculating ISD, the time gap for a passenger car turning left onto a two lane major road is recommended to be 7.5 seconds and 8.0 seconds for a four-lane major road (AASHTO 2011). For the ISD calculation, a time gap of 7.5 seconds was used. The calculated ISD for the intersection of Jefferson and 9th was 83.89 meters (275.63 feet).

A.3 Measured SSD and ISD

The SD was measured in the field at every approach at the intersection of SW Jefferson Way and SW 9th Street.

A.3.1 North Approach

Figure A.2 shows the orientation of Approach 1 and the placement of the objects for the ISD measurement (cones). Table A.1 shows the recorded SD for each object (cones) for Approach 1 (cones placed in North approach).
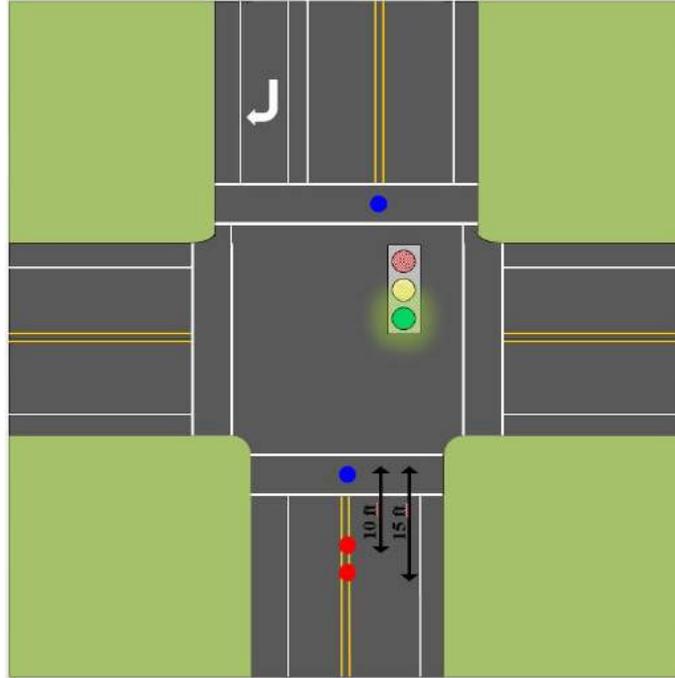
Figure A.2: SD measurement Approach 1

Table A.1 SD measurements Approach 1 (cones placed in North Approach)

Sight Distance Measurement		
Approach 1 (cones are placed in North approach)		
Number of Lanes:	1	
Grade:	-	
Posted Speed:	25 mph	
SSD Measurement	279'	
Measuring SD to the left		
Object	Measurement	Type of Obstruction
1	337	Tree
2	428	Tree
3	297	Tree
4	271	Tree
Measuring SD to the right		
Object	Measurement	Type of Obstruction
1	271	Tree
2	320	Tree/Utility Pole
3	294	Tree/Utility Box
4	309	Tree

The measurement for the SSD was greater than the required 151.86 feet for this approach.

Therefore, there is no issue with the SSD at this approach. However, for ISD, object 1 for the

measurements to the left and object 4 for the measurements to the right were less than the

calculated ISD of 275.63 feet. Furthermore, according to ODOT, the sight triangle is clear of

obstructions if the distance measured from the objects is 900 to 1500 feet or more (McKinley

2014). None of the objects provided a distance of 900 to 1500 feet.

A.3.2 Approach 2

Figure A.3 shows the orientation of Approach 2 and the placement of the objects for the

ISD measurement (cones). Table A.2 shows the recorded SD for each object (cones) for

Approach 2 (cones placed in South approach).

Figure A.3 SD measurement Approach 2

61

Table A.2 SD measurements Approach 2 (cones placed in South Approach)

Sight Distance Measurement		
Approach 2 (cones are placed in South approach)		
Number of Lanes:	1	
Grade:	-	
Posted Speed:	25 mph	
SSD Measurement:	681'	
Measuring SD to the left		
Object	Measurement	Type of Obstruction
1	320	Tree/Utility Pole
2	271	Tree
3	511	Tree
4	473	Tree
Measuring SD to the right		
Object	Measurement	Type of Obstruction
1	428	Tree
2	341	Tree
3	363	Vegetation/Fencing
4	330	Vegetation/Fencing

The measurement for the SSD was greater than the required 151.86 feet for this approach. Therefore, there was no issue with the SSD at this approach. However, for ISD, object 2 for the measurements to the right was less than the calculated ISD of 275.63 feet. Furthermore, none of the objects provided a distance of 900 to 1500 feet, and therefore, the sight triangle was not clear of obstructions according to the ODOT procedure (McKinley 2014).

A.3.3 Approach 3

Figure A.4 shows the orientation of Approach 3 and the placement of the objects for the
ISD measurement (cones). Table 3.3 shows the recorded SD for each object (cones) for
Approach 3 (cones placed in East approach).

Figure A.4 SD measurement Approach 3

Table A.3 SD measurements Approach 3 (cones placed in East Approach)

Sight Distance Measurement		
Approach 3 (cones are placed in East Approach)		
Number of Lanes:	1	
Grade:	-	
Posted Speed:	25 mph	
SSD Measurement:	633	
Measuring SD to the left		
Object	Measurement	Type of Obstruction
1	485	Tree/Utility
2	669	Tree
3	363	Tree
4	296	Tree
Measuring SD to the right		
Object	Measurement	Type of Obstruction
1	137	Tree/Utility
2	235	Tree
3	234	Tree
4	217	Tree

The measurement for the SSD was greater than the required 151.86 feet for this approach. Furthermore, for ISD, all of the objects measured to the right were less than the calculated ISD of 275.63 feet. Additionally, none of the objects provided a distance of 900 to 1500 feet, and therefore, the sight triangle was not clear of obstructions according to the ODOT procedure (McKinley 2014).

A.3.4 Approach 4

      Figure A.5 shows the orientation of Approach 4 and the placement of the objects for the

ISD measurement (cones). Table A.4 shows the recorded SD for each object (cones) for

Approach 4 (cones placed in West approach).
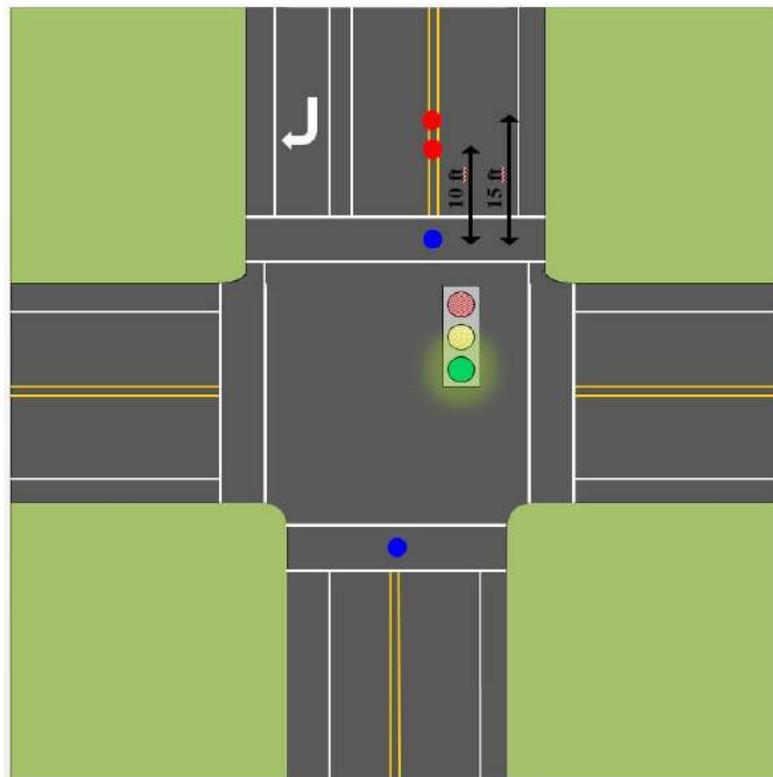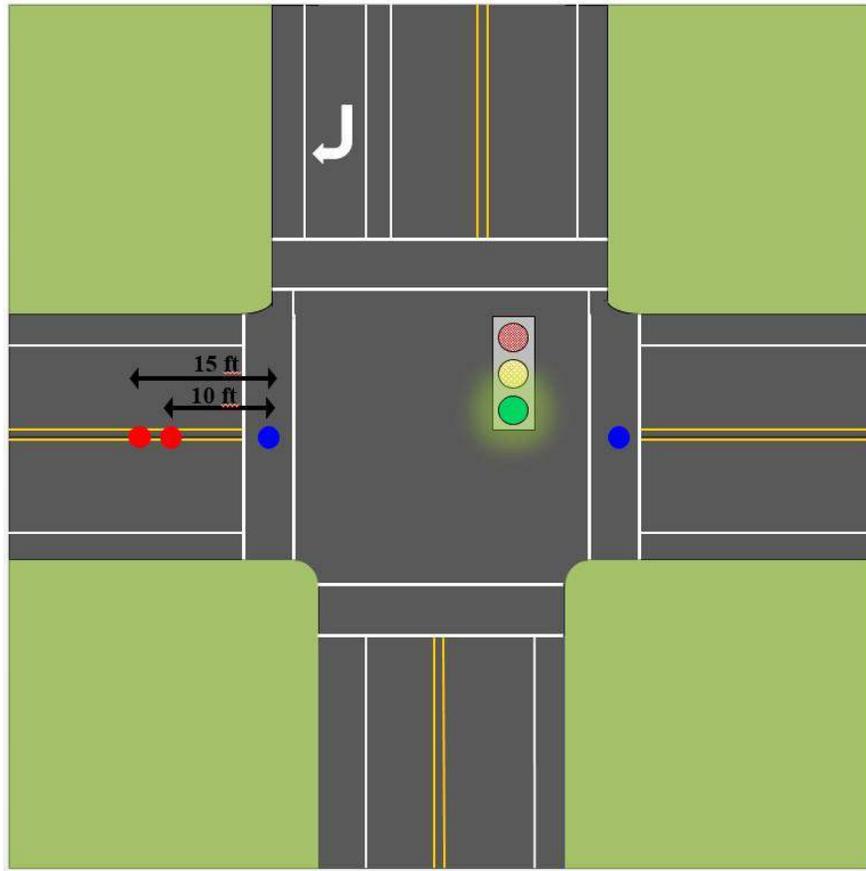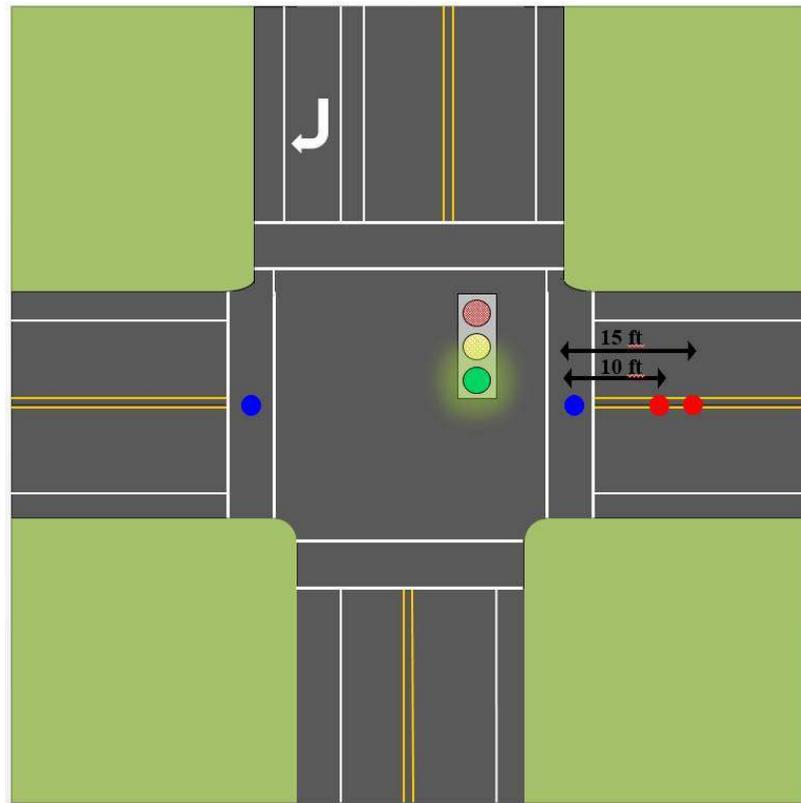

Figure A.5 SD measurement Approach 4

Table A.4 SD measurements Approach 4 (cones placed in West Approach)

Sight Distance Measurement		
4Approach (cones are placed in West approach)		
Number of Lanes:	1	
Grade:	-	
Posted Speed:	25 mph	
SSD Measurement:	1380'	
Measuring SD to the left		
Object	Measurement	Type of Obstruction
1	231	Tree
2	137	Utility Box
3	330	Tree
4	205	Tree
Measuring SD to the right		
Object	Measurement	Type of Obstruction
1	669	Tree
2	485	Utility Pole
3	600	Tree
4	459	Tree

The measurement for the SSD was greater than the required 151.86 feet for this approach. Therefore, there was no issue with the SSD at this approach. Furthermore, for ISD, all of the objects measured to the left were less than the calculated ISD of 275.63 feet. Additionally, none of the objects provided a distance of 900 to 1500 feet, and therefore, the sight triangle was not clear of obstructions according to the ODOT procedure (McKinley 2014).

A.6 Summary

Table A.5 provides a SD analysis summary for the study conducted at SW Jefferson Way and SW 9th Street. The required SSD and ISD measurements were based on the requirements provided by AASHTO for a design speed of 25mph (AASHTO 2011). The measurement used for the ISD for each approach was the smallest distance measured to the right. This is because

AASHTO uses the measurement to the right to create sight triangles. The smallest measurement is used for comparison in order to be conservative and guarantee the safety of the intersection. Furthermore, AASTHO states, "if the available [ISD] for an entering or crossing vehicle is at least equal to the appropriate [SSD] for the major road, then drivers have sufficient [SD] to anticipate and avoid collisions" (AASHTO 2011). This was the case for all ISD measurements in comparison to the required and calculated SSD. However, this is not the case when compared with the measured SSD.

Table A.5 SD analysis summary for the SW Jefferson Way and SW 9th Street intersection

Approach	Stopping Sight Distance (ft)			Intersection Sight Distance (ft)		
	Required	Calculated	Measured	Required	Calculated	Measured
Northbound	155	151.86	279	275.6	275.63	294
Southbound	155	151.86	681	275.6	275.63	330
Eastbound	155	151.86	633	275.6	275.63	217
Westbound	155	151.86	681	275.6	275.63	459

On the basis of the data collected, the intersection had sufficient SSD and ISD for most approaches, with the exception of Approach 3, which did not provide adequate ISD. Therefore, mitigation for intersection obstructions would need to be applied in order for Approach 3 to meet the requirements for ISD.

Appendix B: Spot Speed Study at SW Jefferson Ave and SW 9th St

To conduct the spot speed field study, the observer was located approximately 500 feet up/downstream of the intersection of SW Jefferson Ave and SW 9th St at the designated approach. Between 50 and 100 vehicles were observed per approach. A Pocket Radar device was used to measure the speeds of the vehicles. All vehicles were free flowing vehicles. Free flow speed is defined as "the speed when there are no constraints placed on a driver by other vehicles on the road" (Hall, n.d.). Tables B.1, B.2, B.3, and B.4 show the data collected at the site.

Once the data had been collected, speed groups, frequencies, and cumulative frequencies (tables B.5, B.6, B.7, and B.8) were calculated for all approaches and plotted (figures B.1, B.2, B.3, and B.4).   The mean, median, mode, range, standard deviation, 85th percentile, and speed range (pace of traffic) were calculated (tables B.9, B.10, B.11, and B.12). These statistics were calculated for all approaches for the entire data set, as well as subdivided for passenger cars (PC), light trucks (LT), trucks (T), and semi-trucks (ST).

Table B.1: North Approach data collection

Spot Speed Study Data Collection Form							
Location: SW Jefferson Ave & SW 9th St				Observer: Kamilah Buker			
Date: 08/10/15		Time: 2:30PM to 4:20PM		Direction of Travel: North		Posted Speed: 25 mph	
Weather Conditions: Partly Cloudy				Length of Trap: NA			
Speed (mph)	Veh Class	Speed (mph)	Veh Class	Speed (mph)	Veh Class	Speed (mph)	Veh Class
20	PC	23	PC	20	PC		
23	PC	24	PC	21	LT		
22	PC	23	PC	22	PC		
26	PC	23	PC				
23	PC	20	PC				
20	PC	21	PC				
24	PC	25	PC				
26	PC	22	PC				
29	PC	25	PC				
24	LT	23	PC				
32	PC	25	LT				
27	PC	35	PC				
30	PC	20	PC				
22	LT	22	PC				
20	PC	23	PC				
23	PC	23	PC				
22	PC	22	M				
24	PC	23	LT				
26	PC	24	PC				
33	LT	27	PC				
28	PC	23	PC				
24	LT	21	PC				
27	PC	24	PC				
26	PC	23	PC				
25	LT	24	PC				

Table B.2: South Approach data collection

Spot Speed Study Data Collection Form							
Location: SW Jefferson Ave & SW 9th St				Observer: Kamilah Buker			
Date: 08/11/15		Time: 8:20AM to 10:20AM		Direction of Travel: South		Posted Speed: 25 mph	
Weather Conditions: Sunny				Length of Trap: NA			
Speed (mph)	Veh Class	Speed (mph)	Veh Class	Speed (mph)	Veh Class	Speed (mph)	Veh Class
27	PC	25	LT	26	PC	20	LT
26	PC	23	PC	24	PC	20	T
23	PC	23	LT	27	PC	23	PC
23	LT	25	PC	24	PC	24	PC
24	PC	23	PC	25	PC	22	PC
25	LT	29	PC	20	PC	26	PC
26	PC	23	LT	19	B	31	PC
27	PC	24	PC	23	PC	24	PC
27	PC	23	LT	24	PC	30	M
23	PC	21	T	23	PC	22	PC
24	PC	24	PC	22	PC	25	PC
26	PC	26	PC	24	PC	24	PC
22	PC	22	LT	25	PC	24	PC
30	PC	24	PC	25	LT	25	PC
20	LT	23	PC	25	PC	24	ST
22	PC	28	PC	24	PC	27	PC
27	PC	22	PC	25	PC		
27	PC	27	PC	24	LT		
21	PC	23	LT	25	PC		
21	PC	24	PC	24	LT		
23	LT	22	PC	24	LT		
19	T	24	PC	25	PC		
41	PC	23	PC	23	PC		
26	PC	23	LT	21	PC		
21	PC	22	PC	21	PC		

Table B.3: East Approach data collection

Spot Speed Study Data Collection Form							
Location: SW Jefferson Ave & SW 9th St				Observer: Kamilah Buker			
Date: 08/11/15		Time: 02:45PM to 4:45PM		Direction of Travel: East		Posted Speed: 25 mph	
Weather Conditions: Sunny and Partly Cloudy				Length of Trap: NA			
Speed (mph)	Veh Class	Speed (mph)	Veh Class	Speed (mph)	Veh Class	Speed (mph)	Veh Class
23	PC	24	PC	27	PC	32	PC
20	PC	25	PC	24	PC	25	PC
25	PC	22	PC	25	PC	24	PC
31	PC	28	PC	25	PC	30	PC
21	PC	26	PC	26	PC	25	PC
21	PC	24	PC	25	PC	29	B
24	PC	30	PC	27	PC	28	PC
28	PC	25	PC	34	LT	28	PC
29	PC	29	M	24	PC	26	PC
22	PC	22	LT	30	PC	31	PC
22	PC	34	LT	32	PC	24	PC
28	PC	27	PC	29	PC	25	PC
25	PC	25	LT	22	LT	26	PC
25	PC	21	LT	24	PC	33	PC
25	PC	23	LT	28	PC	28	LT
25	B	28	LT	26	PC	24	PC
23	LT	22	LT	31	PC	23	PC
27	PC	26	LT	24	LT	26	PC
24	PC	23	PC	29	PC	24	PC
22	PC	27	PC	27	PC	25	PC
28	PC	28	B	25	PC	23	LT
25	PC	31	LT	26	LT	32	PC
32	PC	25	PC	33	PC	24	PC
22	PC	34	PC	31	PC	26	LT
26	PC	24	PC	26	PC	23	PC

Table B.4: West Approach data collection

Spot Speed Study Data Collection Form							
Location: SW Jefferson Ave & SW 9th St				Observer: Kamilah Buker			
Date: 08/12/15		Time: 7:40AM to 9:30AM		Direction of Travel: West		Posted Speed: 25 mph	
Weather Conditions: Sunny and Partly Cloudy				Length of Trap: NA			
Speed (mph)	Veh Class	Speed (mph)	Veh Class	Speed (mph)	Veh Class	Speed (mph)	Veh Class
34	PC	25	PC	31	PC	30	PC
22	PC	28	PC	25	PC	25	PC
28	PC	25	LT	30	PC	24	PC
31	PC	26	PC	28	PC	24	LT
25	LT	26	PC	29	PC	25	PC
27	PC	26	LT	28	PC	29	PC
25	PC	29	PC	21	B	30	PC
26	PC	27	PC	27	PC	25	PC
23	PC	24	PC	25	PC	28	PC
29	PC	29	PC	36	PC	28	PC
27	PC	26	PC	30	PC	22	LT
25	PC	26	B	25	PC	24	PC
25	PC	24	B	25	PC	24	PC
24	T	25	PC	31	PC	30	PC
29	PC	28	PC	30	PC	25	PC
26	PC	28	PC	27	LT	22	LT
25	PC	24	PC	27	PC	23	PC
25	PC	25	PC	34	LT	25	PC
23	PC	24	PC	27	M	27	PC
27	B	31	PC	31	PC	24	PC
33	PC	27	PC	24	LT	23	PC
26	PC	25	LT	27	PC	26	T
27	PC	30	PC	25	B	21	PC
27	PC	31	LT	27	PC	36	PC
23	LT	30	LT	26	PC	25	PC

Table B.5 North spot speeds data analysis

Location: SW Jefferson Ave & SW 9th St			Direction: North	Date: 08/12/15
Date of Observations: 08/10/15			Analyst: Kamilah Buker	
Speed Groups	Number Observed	Frequency (%)	Cumulative Frequency (%)	Plotted Speed
20	6	11.32	11.32	20
21	3	5.66	16.98	21
22	7	13.21	30.19	22
23	12	22.64	52.83	23
24	8	15.09	67.92	24
25	4	7.55	75.47	25
26	4	7.55	83.02	26
27	3	5.66	88.68	27
28	1	1.89	90.57	28
29	1	1.89	92.45	29
30	1	1.89	94.34	30
32	1	1.89	96.23	32
33	1	1.89	98.11	33
35	1	1.89	100.00	35
Total	**53**	**100**	-	-
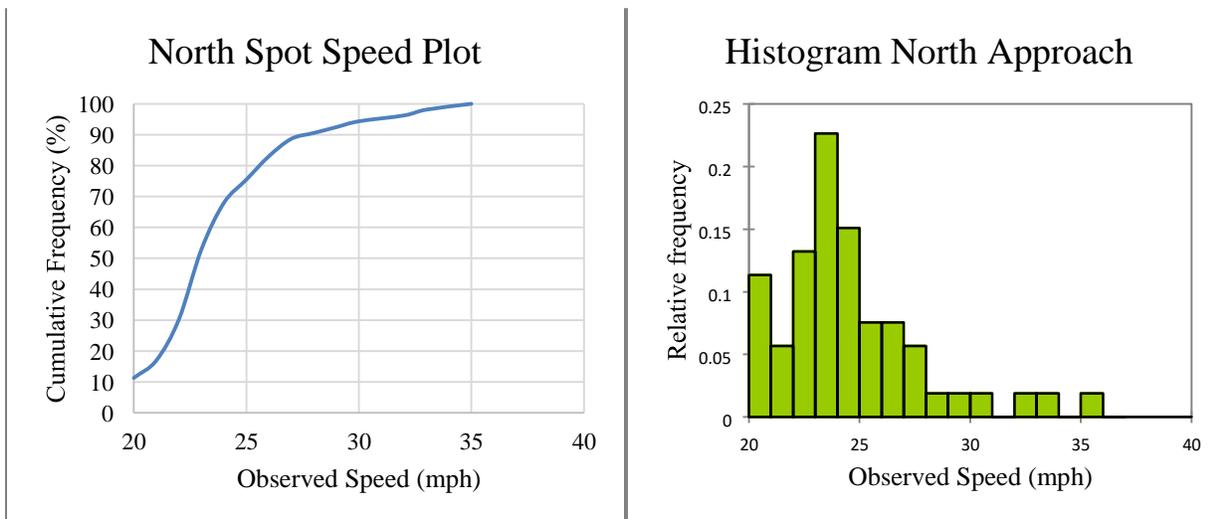
Figure B.1 North spot speed plot and histogram

Table B.6 South direction spot speeds data analysis

Location: SW Jefferson Ave & SW 9th St		Direction: South	Date: 08/12/15
Date of Observations: 08/11/15		Analyst: Kamilah Buker	
Speed Groups	Number Observed	Frequency (%)	Cumulative Frequency (%)	Plotted Speed
19	2	2.20	2.20	19
20	4	4.40	6.59	20
21	6	6.59	13.19	21
22	9	9.89	23.08	22
23	17	18.68	41.76	23
24	20	21.98	63.74	24
25	12	13.19	76.92	25
26	7	7.69	84.62	26
27	8	8.79	93.41	27
28	1	1.10	94.51	28
29	1	1.10	95.60	29
30	2	2.20	97.80	30
31	1	1.10	98.90	31
41	1	1.10	100.00	41
Total	**91**	**100**	-	-
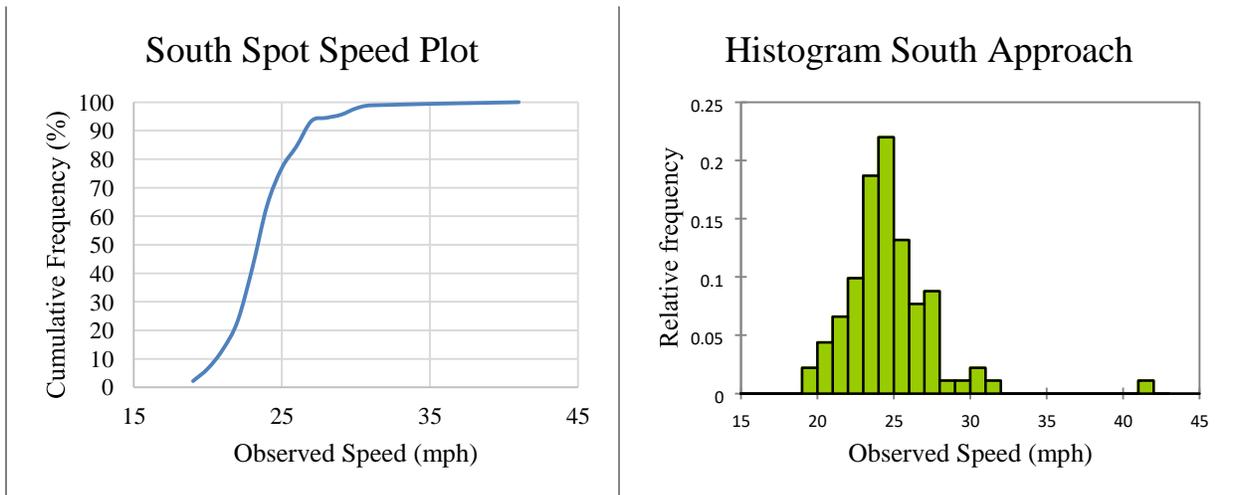
Figure B.2 South spot speed plot and histogram

Table B.7 East direction spot speeds data analysis

Location: SW Jefferson Ave & SW 9th St			Direction: East	Date: 08/12/15
Date of Observations: 08/11/15			Analyst: Kamilah Buker	
Speed Groups	Number Observed	Frequency (%)	Cumulative Frequency (%)	Plotted Speed
20	1	1	1	20
21	3	3	4	21
22	8	8	12	22
23	7	7	19	23
24	14	14	33	24
25	18	18	51	25
26	11	11	62	26
27	6	6	68	27
28	10	10	78	28
29	5	5	83	29
30	3	3	86	30
31	5	5	91	31
32	4	4	95	32
33	2	2	97	33
34	3	3	100	34
Total	**100**	**100**	-	-
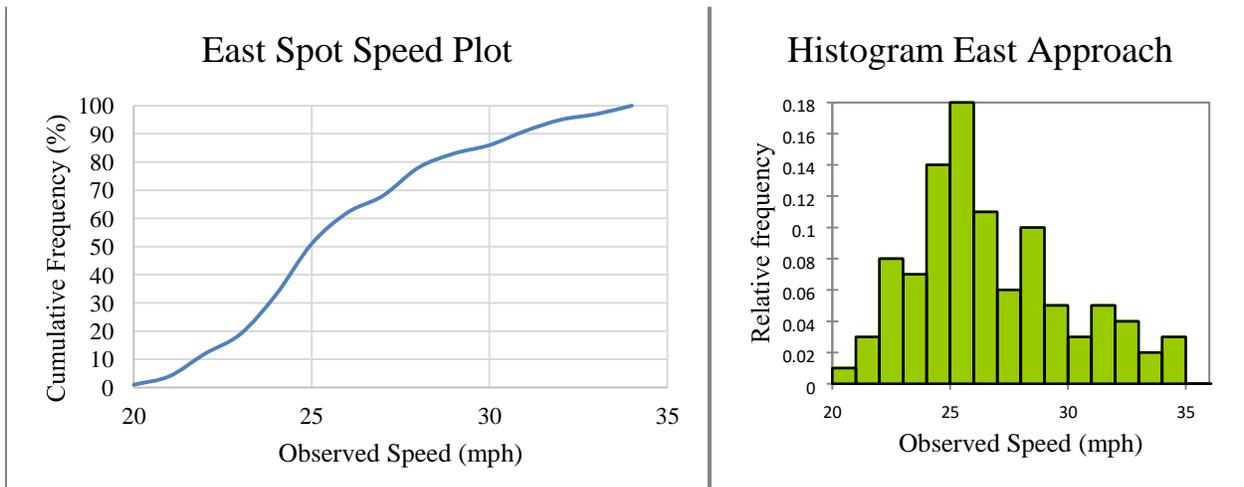
Figure B.3 East spot speed plot and histogram

75

Table B.8 West data analysis

Location: SW Jefferson Ave & SW 9th St			Direction: West	Date: 08/12/15
Date of Observations: 08/12/15			Analyst: Kamilah Buker	
Speed Groups	Number Observed	Frequency (%)	Cumulative Frequency (%)	Plotted Speed
21	2	2	2	21
22	3	3	5	22
23	5	5	10	23
24	11	11	21	24
25	22	22	43	25
26	10	10	53	26
27	14	14	67	27
28	8	8	75	28
29	6	6	81	29
30	8	8	89	30
31	6	6	95	31
33	1	1	96	33
34	2	2	98	34
36	2	2	100	36
Total	**100**	**100**	-	-
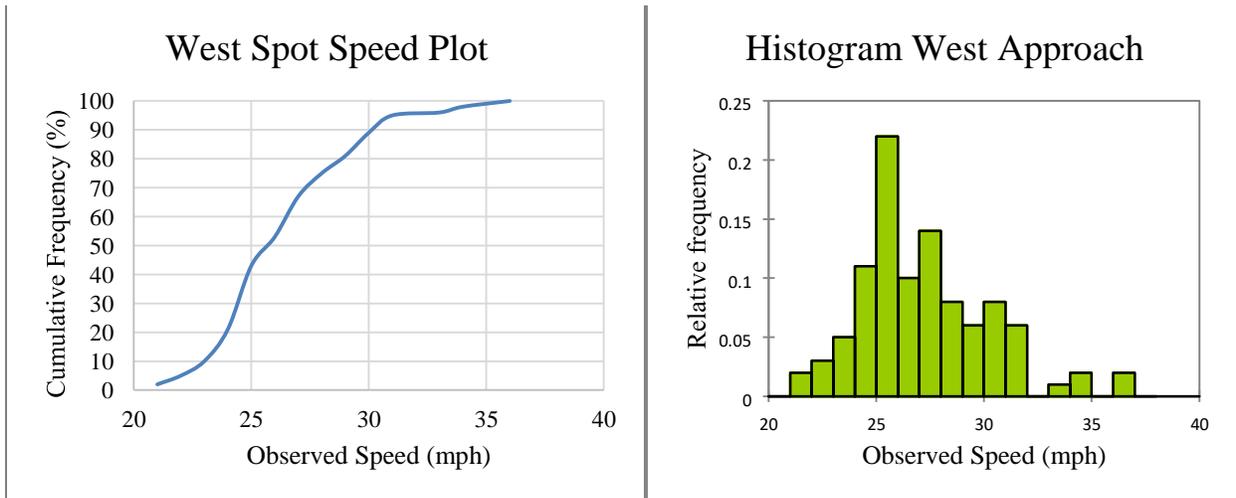
Figure B.4 West spot speed plot and histogram

Table B.9 Spot speed statistics for North direction

North Approach			
	All Vehicles	Passenger Cars	Light Trucks
Mean	**24.09**	24.05	24.63
Median (50th Percentile)	**23.00**	23.00	24.00
Mode	**23.00**	23.00	24.00
Range	**7.50**	7.50	6.00
Standard Deviation	**3.26**	3.24	3.66
85th Percentile	**27.00**	27.00	25.00
Speed Range (Pace)	**18 to 28**	18 to 28	19 to 29

Table B.10 Spot speed statistics for South direction

South Approach				
	All Vehicles	Passenger Cars	Light Trucks	Trucks
Mean	**24.18**	24.59	23.13	20
Median (50th Percentile)	**24.00**	24.00	23.00	20
Mode	**24.00**	24.00	23.00	#N/A
Range	**11.00**	10.50	2.50	1
Standard Deviation	**2.95**	2.98	1.50	1
85th Percentile	**26.50**	27.00	24.75	20.7
Speed Range (Pace)	**19 to 29**	19 to 29	18 to 28	15 to 25

Table B.11 Spot speed statistics for East direction

East Approach				
	All Vehicles	Passenger Cars	Light Trucks	Bus
Mean	**26.20**	26.22	25.76	27.33
Median (50th Percentile)	**25.00**	25.00	25.00	28.00
Mode	**25.00**	25.00	23.00	#N/A
Range	**7.00**	7.00	6.50	2.00
Standard Deviation	**3.29**	3.16	4.07	2.08
85th Percentile	**30.00**	30.00	29.80	28.70
Speed Range (Pace)	**20 to 30**	20 to 30	20 to 30	23 to 33

Table B.12 Spot speed statistics for West direction

	All Vehicles	Passenger Cars	Light Trucks	Trucks	Bus
West Approach					
Mean	**26.72**	27.01	26.00	25.00	24.60
Median (50th Percentile)	**26.00**	27.00	25.00	25.00	25.00
Mode	**25.00**	25.00	24.00	#N/A	#N/A
Range	**7.50**	7.50	6.00	1.00	3.00
Standard Deviation	**3.04**	2.97	3.63	1.41	2.30
85th Percentile	**30.00**	30.00	30.20	25.70	26.40
Speed Range (Pace)	**21 to 31**	22 to 32	20 to 30	20 to 30	20 to 30